1
The Physical Origin of Covalent Bonding

Michael W. Schmidt, Joseph Ivanic, and Klaus Ruedenberg

> ''I believe the chemical bond is not so simple as some people seem to think.''
> Robert S. Mulliken as quoted approvingly by Charles A. Coulson
> *Reviews Modern Physics* ***32****, 177 (1960)*

1.1
The Quest for a Physical Model of Covalent Bonding

Up to about the seventeenth century atomists believed that there were mechanical hookups between atoms. Toward the end of that century Isaac Newton surmised that, analogous to the gravitational forces between masses, there are additional forces between atoms that are attractive at large distances and repulsive at short distances. Around 1810 Berzelius, involved in the development of electrolysis using Volta's recently discovered direct current, conjectured bonding to be due to electrostatic forces by virtue of the same permanent positive or negative charge being distributed on each atom of an element (e.g., H^+, O^-). However, in 1811 Avogadro proposed molecules like H_2 and O_2 to account for volume relationships in gas reactions, a hypothesis that implied the existence of other kinds of bonding forces between atoms. His view was confirmed by the mid-nineteenth century through the development of organic chemistry, which established what is now called *covalent bonding* [1]. In 1881 Helmholtz raised the question of how long-range electrostatic interactions could give rise to short-range bonding forces [2]. After Thomson's discovery of the electron in 1897, it was widely assumed that electrons were involved in bonding. On the basis of chemical evidence, Abegg [3] identified in 1904 what are now called positive and negative oxidation states and deduced that their maximal positive and negative values add up to 8 for each element in the second and third row of the periodic table. He inferred essentially that a special stability must be associated with an electron octet around an atom. Presuming this stability to be a driving force, in 1916 Kossel [4] rationalized ionic bonding by electron transfer whereas, also in 1916, Lewis [5] posited that covalent bonds are achieved by electron sharing.

The Chemical Bond: Fundamental Aspects of Chemical Bonding, First Edition.
Edited by Gernot Frenking, Sason Shaik.

In 1927, Heitler and London [6] showed that wave mechanics yields the covalent bond in the hydrogen molecule whereas Burreau [7] obtained covalent binding for the hydrogen molecule ion. In the subsequent years, these two systems were calculated with increasing accuracy, culminating in the work of James and Coolidge [8] who, in 1933, obtained the binding energy of H_2 within 0.6 kcal mol^{-1}. Today we know that wave mechanics does indeed yield chemical bonding in all molecules for which sufficiently accurate calculations have been made.

However, while the connection between calculation and conceptual physical reasoning is direct and immediate in classical mechanics, this is no longer the case in quantum mechanics. The question arose, therefore, how *conceptual physical reasoning* can be associated with the bond formation that is found in wave mechanical *computations*. Several intuitive answers to this question were proposed in the thirties. From a rather formalistic point of view, bonding was attributed to postulated ‘‘exchange forces.’’ By analogy with the coupling of pendulums, ‘‘resonance’’ effects were posited. The recognition that bonding is associated with an accumulation of charge in the bond region led to the conjecture that the electrostatic attraction between this accumulated charge and the adjacent nuclei generates the lowering of the energy. This suggestion by Slater [9] seemed moreover to be in accordance with the virial theorem, which states that the potential energy decreases and the kinetic energy increases upon bond formation. Hellmann [10], on the other hand, advanced the view that bonding is caused by the lowering of the kinetic energy that results from electrons being able to roam over a larger area in a molecule than in an atom, similar to the effect of increasing the box length for a particle in a box. (He could not reconcile, however, the apparent inconsistency of this explanation with the virial theorem.) None of these conceptual conjectures were rigorously pursued in quantitative detail.

The present approach follows the theoretical tradition that, when a rigorous fundamental mathematical formulation with verified quantitative implications exists, then the choice of explanatory physical concepts is limited by having to reflect closely the relationships that are inherent in the theoretical framework. For the present problem, the challenge is to cast the exact energy expression, generated by accurate electronic wave functions, in a form that allows a rigorous resolution into physically interpretable parts and to find a fundamental principle that guides their interactions. The first coherent analysis of this kind was advanced and applied in the 1960s by one of the present authors and his coworkers [11]. It was based on an energy decomposition analysis of general *ab initio* wave functions of electrons in molecules and it identified the physical interactions that establish the bonds in H_2 and H_2^+. This line of reasoning was subsequently pursued by a number of authors [12]. Recent work by two of the present authors [13] as well as by Bacskay and Nordholm [14] has shed additional light on the problem.

In the present chapter, this approach is developed further. It is then used to examine the covalent bonds of H_2^+ and H_2 in detail and extended to the many-electron molecules B_2, C_2, N_2, O_2, and F_2. These analyses show that covalent bonding involves a synergism between several interactions with quite different physical attributes and quantitative characteristics. On the one hand, the lowering of the energy that establishes the bond is the result of a variational competition between the kinetic energy and potential energy. On the other hand, there occurs an intricate interplay between various intra-atomic and interatomic interactions. These basic agents have, moreover, to accommodate electron correlation. It emerges that, in all cases, the driving force of covalent bond formation is the lowering of the kinetic energy gained by the delocalization of electronic waves over more than one atom. This observation is only superficially discordant with the virial theorem which, as mentioned earlier, requires the molecule to have a higher total kinetic energy than the separated atoms. The in-depth accounting of all interconnections between the various interactions shows that the information disclosed by the *actual* total kinetic and potential energies *per se* is insufficient for drawing any inferences regarding the *origin* of covalent bonding.

1.2
Rigorous Basis for Conceptual Reasoning

The aim of the present analysis is to understand bonding features of potential energy surfaces (PESs), that is, the Born–Oppenheimer separation is assumed. Although the study is limited to ground states, the reasoning also applies to excited states when the consequences of the additional constraints of orthogonality to the lower states are accounted for.

1.2.1
Physical Origin of the Ground State

Bonding on a PES is a consequence of the *geometry dependence* of the electronic energy, specifically that this energy is lower for the molecular equilibrium geometry than for the separated atoms. Therefore, *the first objective must be to develop a conceptual understanding of the physical factors that determine the ground state energy of a system of electrons in the electrostatic field generated by fixed nuclei.*

A rigorous quantum mechanical basis for such an understanding is provided by the variation principle which states that, for all possible normalized electronic wave functions Ψ, the energy integral

$$\mathbf{E}(\Psi) = \int d\tau\, \Psi \mathscr{H} \Psi = \int d\tau\, \Psi \mathscr{T} \Psi + \int d\tau \Psi \mathscr{V} \Psi = \mathbf{T}(\Psi) + \mathbf{V}(\Psi) \qquad (1.1)$$

assumes the *lowest possible* value when Ψ is the ground state Ψ_g. Here, $\mathscr{T}$ and $\mathscr{V}$ are the kinetic and potential energy operators. Hence:

> The shape of Ψ_g is determined by the adjustments needed to minimize $\mathbf{T}(\Psi) + \mathbf{V}(\Psi)$.

The conceptual physical interpretation of $\mathbf{V}$ is self-evident: Its terms represent electron nuclear attractions, electron–electron repulsions and internuclear repulsions, all of which are classical electrostatic concepts. In systems with *bound* electrons the electron nuclear attractions dominate the potential energy integral **V**, which is therefore negative. Manifestly,

> The negative potential energy **V** is lowered by localizing Ψ in regions of low $\mathcal{V}$, in particular by contracting Ψ towards the nuclei.

It is with regard to the kinetic energy ***T*** *that quantum mechanics differs fundamentally from classical mechanics* and that a new type of concept has to be added to the physical reasoning. To this end, it is advantageous to transform the kinetic energy integral **T** into the form:

$$\mathbf{T} = \int \mathrm{d}\tau\, \Psi \mathcal{T}\, \Psi = -\frac{1}{2}\sum_k \int \mathrm{d}\tau\, \Psi(\nabla_k)^2\Psi = +\frac{1}{2}\sum_k \int \mathrm{d}\tau\, (\nabla_k \Psi)^2 \tag{1.2}$$

where the sum $\sum_k$ goes over all electrons k. (Atomic units are used.) If Ψ is expressed in terms of its natural orbitals ψ_n and occupation numbers N_n, then **T** becomes

$$\mathbf{T} = -\frac{1}{2}\sum_n N_n \int \mathrm{d}\tau\, (\psi_n \nabla^2 \psi_n) = \frac{1}{2}\sum_n N_n \int \mathrm{d}\tau\, (\nabla \psi_n)^2 \tag{1.3}$$

The general derivations and conclusions in the subsequent analyses do not depend on whether the Laplacian or the gradient form of **T** is used because only the invariant integrated expectation values are involved in the inferences. In the equations, though, the gradient expression will be preferred for didactic reasons as a positive kinetic energy term always appears with a positive sign in the formulas. In some instances, the gradient expression will, moreover, prove elucidative for understanding properties of certain kinetic energy integrals by relating them to properties of the wave function. This is because, in the gradient expression of Eq. (1.2), *every* electron k makes a *positive* contribution to *every* volume element $\mathrm{d}\tau$, namely *the square of the gradient of* Ψ with respect to the individual electron coordinates. Analogously, in the gradient expression of Eq. (1.3), every orbital makes a positive contribution to every volume element. Most notably, the following fundamental property of the kinetic energy is readily deduced from these attributes of the gradient form.

Consider a single electron where $\Psi = \psi$ and

$$\mathbf{T} = \frac{1}{2}\int \mathrm{d}\tau\, (\nabla\psi)^2 = \frac{1}{2}\int \mathrm{d}x \int \mathrm{d}y \int \mathrm{d}z \left[\left(\frac{\partial\psi}{\partial x}\right)^2 + \left(\frac{\partial\psi}{\partial y}\right)^2 + \left(\frac{\partial\psi}{\partial z}\right)^2\right] \tag{1.4}$$

The following is manifest from this expression. When ψ is squeezed into a smaller space, then the normalization condition $\int \mathrm{d}\tau\, \psi^2 = 1$ requires that the maximum of ψ increases and, consequently, that the average of the gradient of ψ increases. Hence, localizing ψ will increase **T**. This inference is related to the uncertainty relation, which is derived in quantum mechanics texts. By virtue of the additive decomposition (Eq. (1.3)), this correlation is general and fundamental:

> Localizing an electronic wave function increases its positive kinetic energy. In the context of the variation principle, electrons therefore possess an innate drive towards delocalizing the wave function.

It is apparent that the kinetic energy and the potential energy place *opposing demands* on the wave function with regard to the aim of minimizing the total energy $\mathbf{E} = \mathbf{T} + \mathbf{V}$: The kinetic energy would be minimized (viz $\rightarrow 0$) by ultimate dilution of Ψ, and the potential energy would be minimized (viz $\rightarrow -\infty$) by complete concentration onto the nuclear centers. Hence,

> The variational energy minimum is reached by that wave function Ψ_g that achieves the optimal compromise in the variational competition between the electrostatic potential energy pull, which favors localizing contraction towards the nuclei, and the kinetic energy pressure, which drives towards delocalizing dilution.

The *variational process* can therefore be summarized as follows:

> The ground state wave function is determined by the electrostatic attractions pulling the electron cloud as close towards the nuclei as permitted by the resistance of the kinetic energy.

An additional constraint exists in the case of many electrons in that the wave function Ψ must then be antisymmetric with respect to the exchange of electrons, which entails the restriction:

> The simultaneous localization of several electrons in the same space is curbed by the exclusion principle.

It should be appreciated that the quantum mechanical variation principle for the *energy*, that is, $(\mathbf{T} + \mathbf{V})$, lends itself more easily to conceptual visualization than the variation principle of least action, that is, $\int \mathrm{d}t(\mathbf{T} - \mathbf{V})$, does in classical mechanics. This vantage may be considered a compensation for the absence of the kind of direct simple conceptual physical interpretation of calculations that classical mechanics offers.

1.2.2
Physical Origin of Ground State Energy Differences

The prototype example for the described variational competition is the case of an electron-like particle of mass m in the field of a nucleus of charge Z with the Hamiltonian $\mathscr{H} = -(1/2m)\nabla^2 - Z/r$. Consider the normalized trial wavefunction

$$\psi = 1\mathrm{s}_\zeta = \left(\frac{\zeta^3}{\pi}\right)^{\frac{1}{2}} \exp(-\zeta r) = \left(\frac{1}{\alpha^3 \pi}\right)^{\frac{1}{2}} \exp\left(\frac{-r}{\alpha}\right) \qquad (1.5)$$

Here, $\mathscr{H}$ and ψ are in atomic units. The parameter $\alpha = 1/\zeta$ is a measure of the localization of the orbital in as much as the sphere with the radius $R = 2\alpha$ includes

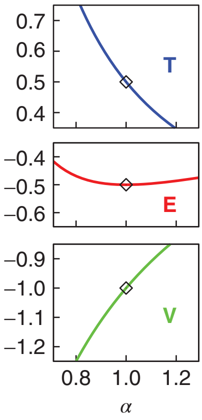

Figure 1.1 Variational competition between kinetic (blue) and potential (green) energies, and the optimal compromise for the total energy (red) that determines the ground state of the hydrogen atom. Ordinate = energy in hartree. Abscissa = orbital size as measured by the inverse orbital exponent $\alpha = 1/\zeta$ in Eq. (1.5).

94% of the orbital density ψ^2. The kinetic and potential energy integrals of ψ become

$$\mathbf{T} = \frac{\zeta^2}{2m} = \frac{1}{2}m\alpha^2 \qquad \mathbf{V} = -\zeta Z = \frac{-Z}{\alpha} \tag{1.6}$$

and they are plotted as functions of the localization parameter α in Figure 1.1. Indeed they exhibit the behavior discussed in the preceding section and the plot of the total energy $(\mathbf{T} + \mathbf{V})$ exhibits the variational competition between $\mathbf{T}$ and $\mathbf{V}$. The minimum, that is, the optimal compromise between these two functions occurs for

$$\zeta_g = mZ, \quad \mathbf{T}_g = \frac{1}{2}mZ^2, \quad \mathbf{V}_g = -mZ^2, \quad \mathbf{E}_g = -\frac{1}{2}mZ^2 \tag{1.7}$$

For the hydrogen atom, where $m = 1$ au and $Z = 1$ au, Eq. (1.7) yields the ionization potential 0.5 hartree. The physical origin of the magnitude of this fundamental quantum chemical quantity is thus the variational compromise between $\mathbf{T}$ and $\mathbf{V}$ in hydrogen.

Atomic energy units will be used in this chapter. The relation to units often used in experimental work is: 1 millihartree = 1 mh = 2.6255 kJ mol^{-1} = 0.62750 kcal mol^{-1}.

Consider now cases with a different nuclear charge Z and a different particle mass m (note, e.g., that the pi-muon has the same charge as the electron but is 180 times heavier) and let us examine *why* such systems can have *lower* ground state energies than the hydrogen atom. From the expression for $\mathbf{E}_g$ in Eq. (1.7) it is apparent that *there can be two different reasons*: (i) The nuclear charge Z is larger than the proton charge or (ii) the mass m of the particle is heavier than the electron mass.

This distinction exhibits an important aspect of the variational competition that is relevant for the elucidation of energy differences between related systems. It is illustrated in Figure 1.2, which shows the variational competition and the shift of the optimal compromise for several systems of the kind described by Eq. (1.6). To

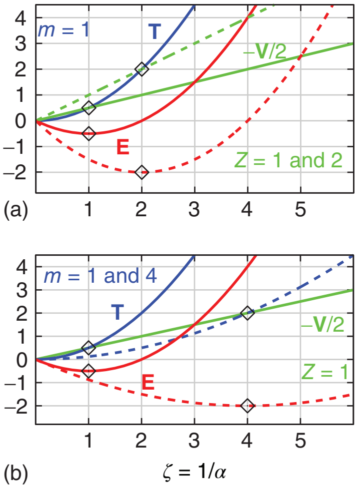

Figure 1.2 Variational competition and optimal compromise between kinetic and potential energies for hydrogen-like systems (see Eq. (1.6)). The solid curves correspond to the standard hydrogen atom, $m=1$ for **T** and $Z=1$ for **V**. The dashed curves of **T**, **V**, and **E** correspond to different choices of m and Z, viz: $Z=2$ for **V** in (a) and $m=4$ for **T** in (b). Abscissa = orbital exponent $\zeta=1/\alpha$, implying the *inverse* of the orbital size. Ordinate = energy in hartree; note that $-\mathbf{V}/2$ is plotted. Diamond markers indicate the positions of the variational compromises.

display clearly the pertinent features, the energies **E**, **T**, and $|\mathbf{V}/2|$ are plotted and the orbital exponent $\zeta=1/\alpha$ is used as abscissa. Consequently, $|\mathbf{V}/2|$ is a straight line and **T** is a quadratic. *Note that, in Eq. (1.7), the minimum of the energy always occurs at that value of* ζ *where* $\mathbf{T}=|\mathbf{V}/2|$*, that is, where the straight line* $|\mathbf{V}/2|$ *intersects the quadratic* **T***. This is a general constraint whose rigorous origin will be discussed in the next section.*

Figure 1.2a shows the cases for $\{m=1,\ Z=1\}$ and $\{m=1,\ Z=2\}$. Changing the nuclear charge Z from 1 to 2 increases the slope of the line $|\mathbf{V}/2|$ so that it intersects the quadratic **T** at a larger value of ζ and a lower energy than in hydrogen. The variational interpretation is as follows: Increasing Z *strengthens the nuclear electrostatic pull*. In the presence of the same kinetic resistance as in hydrogen, the orbital is pulled *closer* to the nucleus than in hydrogen and the energy is thereby lowered.

Figure 1.2b shows the cases $\{m=1,\ Z=1\}$ and $\{m=4,\ Z=1\}$. According to Eq. (1.6), changing the mass m from 1 to 4 decreases the curvature of **T** so that the intersection of $|\mathbf{V}/2|$ with **T** occurs again at a larger value of ζ and a lower energy than in hydrogen. The variational interpretation is now as follows: Increasing the mass *m weakens the kinetic resistance* because the mass is in the denominator of the expression for **T**. Because the nuclear pull is the same as in hydrogen, the orbital is again pulled *closer* to the nucleus than in hydrogen and the energy is again lowered. Thus:

> The difference between the ground state energies of two systems of bound electrons can be due to a difference in the strength of the attraction towards the regions of low potential energy or it can be due to a difference in the strength of the kinetic resistance towards localization in the regions of low potential energy.

It is of course possible that both factors are simultaneously operative.

Moreover, the discussed examples exhibit another important fact. According to Eq. (1.7), the two systems $\{m = 1, Z = 2\}$ and $\{m = 4, Z = 1\}$ have the same values of $\mathbf{E}_g = -2$, $\mathbf{T}_g = 2$ and $\mathbf{V}_g = -4$ hartree. These equalities show that it is *not* possible to tell *why* either of these systems has a lower energy than hydrogen when the *only* information available are the values of $\mathbf{E}_g$, $\mathbf{T}_g$, and $\mathbf{V}_g$. Thus,

> An analysis of the physical origin of energy differences between systems requires more information than is furnished by the values of $\mathbf{E}_g$, $\mathbf{T}_g$ and $\mathbf{V}_g$.

Indeed, the preceding *variational analysis* on the basis of Figure 1.2 made use of the knowledge of *comparison values* for $\mathbf{E}$, $\mathbf{T}$, and $\mathbf{V}$, in addition to those at the variational minimum.

1.2.3
Relation between Kinetic and Potential Energies

As noted in the preceding section, the optimized kinetic and potential energies of the ground states in these systems always stand in the constant ratio $\mathbf{V}_g/\mathbf{T}_g = -2$. This relationship, which is known as the virial theorem, in fact, holds rigorously for the *many* electron wave functions of *any* atom. It is a general theoretical consequence of the fact that the kinetic energy scales as (inverse length)^2 whereas the potential energy scales as (inverse length). Furthermore, it is important that this relationship is not only valid for the actual solution of the Schrödinger equation (which is optimized with respect to *all possible* variations) but also *for approximate wave functions that are merely optimized with respect to a single scale parameter for all electrons* [15]. If a many-electron wave function is expressed as a superposition of determinants of atomic orbitals (AOs), then *individual* scaling of the various AO exponents will guarantee the virial relation *a fortiori*. When *sufficiently large* basis sets with fixed exponents are employed in a calculation, then the exponential optimization of AOs will be mimicked by the linear combination of atomic orbital (LCAO) expansions of the molecular orbitals (MOs).

In a diatomic molecule, the virial relationship has the general distance-dependent form [9]

$$2\mathbf{T} + \mathbf{V} + R\left(\frac{d\mathbf{E}}{dR}\right) = 0 \tag{1.8}$$

If an approximate molecular wave function is constructed from AOs, say $\chi_{An}[\zeta_{An}(r - R_A)]$, where χ_{An} denotes orbital n on atom A at the position R_A with orbital exponent ζ_{An}, then the general virial theorem results from the following optimization [15]: Replace all orbital exponents by $s\zeta_{\mathrm{An}}$ and optimize with respect to the one global scale parameter s. Again, optimization with respect to *all individual* orbital exponents, or a common scale parameter of groups of orbital exponents, will guarantee the virial relation *a fortiori*. These kinds of scaling manifestly represent *simultaneous shrinking or swelling with respect to all atoms* in the molecule. (Equation (1.8) can be generalized to polyatomic systems.)

It follows from Eq. (1.8) that the relation found for atoms, viz

$$2\mathbf{T} = -\mathbf{V} = |\mathbf{V}| \tag{1.9}$$

is in fact also valid *at all points where the energy gradient vanishes*, notably at equilibrium geometries and transition states. A corollary is that the relation is also valid for energy *differences such as binding energies and activation energies*. At these critical points, the satisfaction of Eq. (1.9) is a simple indicator as to whether a given wave function possesses the following property.

The virial theorem is evidence of the intrinsic balance between the intra-atomic and the interatomic electronic density distributions that is required for the optimal balance in the variational competition between the potential pull of the nuclei and the kinetic resistance of the electron wave. It is a necessary attribute of the actual wave function and thus represents a *constraint* that approximate wave functions must satisfy if successive improvements are to lead to the exact solution. Satisfaction of this constraint by an approximate wave function implies that the optimal compromise between the potential pull and the kinetic resistance has been achieved *within the formal limitation of that wave function*.

By virtue of the response of the kinetic and potential energies to orbital contraction, which was illustrated in Section 1.2.2, one readily infers that, at the critical geometries, the following assessments of an *approximate* wave function Ψ can be made:

If $2\mathbf{T}(\Psi) < |\mathbf{V}(\Psi)|$, then the actual solution Ψ_g is in some way more localized than Ψ.
If $2\mathbf{T}(\Psi) > |\mathbf{V}(\Psi)|$, then the actual solution Ψ_g is in some way less localized than Ψ.

These inequalities are helpful in understanding the changes induced by wave function optimizations.

Because the energy increases quadratically near the variational minimum, certain wave functions that do not satisfy the virial theorem can yield rough approximations to the exact *energy*, as exemplified by the wave function of Heitler and London. However, the flaws in the *wave functions*, as well as other expectation values, are considerably more serious, as exemplified by the manifestly large error in the expectation value of $1/r$.

Notwithstanding its usefulness, it should be noted that – contrary to widespread misconceptions – *the virial theorem per se generates no clues whatsoever* for answering the question *why one system is more stable than another*. This inability is for instance exhibited by the two *isoenergetic* systems $\{m = 1, Z = 2\}$ and $\{m = 4, Z = 1\}$, which were examined in Section 1.2.2. *Both* satisfy the virial theorem but, as discussed there, the two differ radically regarding their physical reasons for being more stable than hydrogen, which also satisfies the virial theorem.

1.3
Atoms in Molecules

1.3.1
Quantitative Bonding Analyses Require Quasi-Atoms in a Molecule

The chemical notion that molecules consist of atoms held together by bonds implies (i) that atoms occur not only as free entities but are also preserved in molecules, albeit possibly deformed, and (ii) that there exist interactions between them that establish the cohesion. To retrieve this model from accurate quantum mechanical wave functions presents a nontrivial challenge because, in fact, chemical binding results from electrons being *shared between several atoms* so that, for instance, very compact wave functions are typically represented in terms of MOs that are delocalized over many atoms, the simplest examples being canonical Hartree–Fock determinants. To recover and identify ''atoms'' in an electronic wave function Ψ requires therefore *a transformation of its representation in such a way that* Ψ *becomes constructed from subunits that exhibit atomic character*. As in previous studies, we denote such atom-like building blocks of Ψ in a molecule as *quasi-atomic*.

Important in the present context is that the expression of molecular electronic wave functions in terms of quasi-atomic components not only gratifies the chemical intuition but that *it is in fact an indispensible prerequisite for developing a rigorous quantitative analysis of the origin of covalent bonding*. This is because *the maximization of the interatomic energy lowering that creates bonding will be seen to entail a deformation of atoms into quasi-atoms.* Since, by virtue of the *atomic* variation principle, such intra-atomic deformations are necessarily antibonding, there exists a subtle competition between the intra-atomic and the bond-creating interatomic energy changes, whose elucidation cannot be bypassed if one wishes to understand the bonding mechanism.

1.3.2
Primary and Secondary Energy Contributions

For the interpretation of chemical bonding, it is helpful as well as physically justified to take into account that the influences determining atomic and molecular electron distributions can be attributed to two kinds of forces. The primary influence is the effective one-electron potential that the nuclei and the average electron distribution generate. The secondary influence is the many-electron potential that is caused by the deviations of the individual interelectronic interactions from the average, that is, the dynamic correlations. The primary potential creates a primary orbital space in which the stock [16] of the ground state wave function takes form. It can be a single-configuration (SCF) or, if several configurations compete energetically, a multi-configurational (MCSCF) function. The secondary potential generates correlation refinements of the wave function that are grafted onto the primary stock. Unfortunately, for historical formal reasons, the label ''correlation,'' albeit ''non-dynamical,'' ''static'' or ''strong,'' is often also used for primary multi-configurational wave functions.

The primary orbital space of an *atom* is spanned by its optimized *minimal basis set orbitals*. This intuitive insight by the pioneers of the 1930s, which provided the basis for their remarkable qualitative successes, has been confirmed by the quantitative *ab initio* work of the computer-age. In the many atoms with open valence shells, that is, where the number of valence electrons is less than twice the number of minimal basis valence orbitals, the primary stock of the ground state wave function is frequently multi-configurational.

The analysis of chemical bonding is greatly clarified by separating the binding effects involving the primary stocks of the atomic wave functions from those involving the dynamic correlations. Bonds between atomic primary stocks form when at least one atom has an open valence shell because, then, the innate delocalization drive will cause at least some valence electrons to use available minimal basis set orbitals on *several* atoms, that is, the kinetic energy will be lowered by ''electron sharing.'' In covalent bonds, this bonding in the primary orbital space typically dominates markedly over the correlation contributions. But even when dynamic correlations play a greater or even an essential part in bonding, separating the two types of contributions greatly clarifies the elucidation.

For these reasons, the bonding analyses of the present study focus primarily on MCSCF wave functions in full valence spaces. As in our earlier work, [17] we denote these *very specific* type of full space MCSCF wave functions as FORS (full optimized reaction space) wave functions. The correlation contributions to covalent bonds will then also be briefly examined.

1.3.3
Identification of Quasi-Atoms in a Molecule

In the present discussions, electronic wave functions are conceived of as being constructed from orbitals. The identification of quasi-atoms in a molecule consists then of two steps: (i) the identification of *quasi-atomic orbitals*, generically denoted as QUAOs, in terms of which the molecular electronic wave function Ψ can be expressed, and (ii) the construction of quasi-atomic *configurations* from these orbitals in terms of which the wave function Ψ can be expanded. The determination of such QUAOs and configurations requires a judicious choice of appropriate localization criteria. We consider it desirable to determine QUAOs and configurations in such a way that they *differ as little as possible from the corresponding free-atom quantities while still being capable of regenerating the molecular wave function*.

For the determination of QUAOs, the following procedure is used in the present analysis. Let ψ_k be the orbitals from which the molecular wave function is constructed, ordered by importance, for example, through a natural orbital expansion. Then the nonsymmetric, usually rectangular, overlap matrix is calculated between these MOs and the full set of orthogonalized atomic basis orbitals used on *one* atom A (such as, e.g., a cc-pVXZ basis). The singular value decomposition (SVD) of this overlap matrix determines a set of *MOs*, that is, linear combinations of the ψ_k, and an equal number of orbitals in the *AO basis space* on atom A. They form corresponding pairs with maximum possible overlap integrals, which are given by the (always positive) singular values of the SVD. This procedure is done for every atom in the molecule. Using the magnitudes of the singular values of the SVDs for the various atoms as guides, a certain number of the SVD-generated MOs is chosen from each atom as QUAOs for that atom, subject to the limitation that the total number of the quasi-atomic orbitals selected for all atoms is equal to the total number of the original MOs ψ_k. This set χ_ν of QUAOs has the following properties:

- It spans the space of the MOs so that the original electronic wave function can be expressed in terms of configurations formed from these quasi-atomic orbitals.
- If a sufficient number of MOs ψ_k are used, then the QUAOs turn out to be essentially localized on the various atoms.
- The QUAOs χ_ν on one atom are mutually orthogonal.
- The QUAOs χ_ν from different atoms are mutually non-orthogonal. If it is expedient for some purpose, they can be symmetrically orthogonalized.

In the case of a full valence space FORS MCSCF wave function, the number of MOs is equal to the total number of conceptual minimal basis set orbitals in the molecule. For any one atom, the number of quasi-atomic orbitals is then chosen to be equal to the number of minimal basis orbitals on that atom. The quasi-atomic orbitals in fact *are* the deformed minimal basis set orbitals on that atom. The abbreviation QUAFO will be used for these quasi-atomic FORS orbitals. The corresponding linear combinations of the atomic basis orbitals on A represent the optimal *pure atomic approximate orbitals* (PAAOs) to the QUAFOs. In the molecules H_2, B_2, C_2, N_2, O_2, F_2 discussed in the following paragraphs, all overlap integrals between the QUAFOs and the corresponding PAAOs are found to be larger than 0.99, which exhibits the atomic character of the QUAFOs. Nonetheless, the PAAOs do not generate the molecular wave function and a close examination shows that the QUAFOs contain small admixtures from other atoms. (Molecular wave functions formed by configuration interaction (CI) calculations using the PAAOs yield energies a few millihartree higher than the FORS wave functions.) Details of the SVD method will become apparent from the explicit applications in the molecules discussed below in the following paragraphs. In the case of F_2, the method is also used for a wave function that includes orbitals providing some dynamic correlation.

An in-depth elaboration and discussion of the SVD approach to generate quasi-atomic orbitals in molecules will be given in a separate investigation [18]. It has been found for instance that, under certain conditions, some correlating orbitals beyond the FORS level are required to achieve satisfactory localization on atoms. On the other hand, for some wave functions, the number of available occupied MOs may be less than the total number of minimal basis set orbitals. There then exists some additional freedom that allows further atomic adaptation of the quasi-atomic orbitals. A systematic approach to this problem has been formulated previously [19] and is also discussed in Ref. [18]. In the case of polyatomic molecules, an unbiased method has furthermore been developed for forming hybrid QUAFOs that clearly exhibit directional bonding on each atom [20].

1.4
The One-Electron Basis of Covalent Binding: H_2^+

The question to be answered is: Why does the optimal compromise between the potential energy pull and the kinetic energy resistance occur for a lower total energy in H_2^+ than in H? In the end, it turns out that the kinetic energy plays the more critical role and that no *static* model can account for the physical origin of binding in H_2^+ and H_2. Furthermore, notwithstanding inner shells and other complicating factors present in atoms beyond helium, covalent bond formation appears to be generally driven by kinetic effects that are analogous to those exemplified in the prototype H_2^+ bond.

To place the analysis of this molecule on the firmest possible footing, it will be deduced from near-exact wave functions [13]. They were obtained in terms of uncontracted (14s, 6p, 3d, 2f, 1g) basis sets of 26 σ-type spherical Gaussian AOs on the two atoms, in which all orbital exponents were optimized. For the hydrogen atom, the energy found in this basis lies 0.1 μh (microhartree) above the exact value, with a virial ratio of $2\mathbf{T}/|\mathbf{V}| = 0.99999985$. The energy of the molecule is found to lie 0.55 μh above the exact value at the equilibrium distance, which is found to be $R = 1.99720$ Bohr. The virial ratio is $2\mathbf{T}/|\mathbf{V}| = 0.9999982$ at this distance [21]. The wave function can be expected to be of similar quality at intermediate distances. The quantitative results on which the discussion of the present section is based have been reported in detail in Ref. [13].

1.4.1
Molecular Wave Function as a Superposition of Quasi-Atomic Orbitals

There are two atomic minimal basis set orbitals in this system. According to the discussion in Section 1.3.2, the molecular FORS space is, therefore, also two-dimensional. However, only the bonding molecular FORS orbital is occupied whereas the second molecular FORS orbital, the antibonding orbital, is unoccupied. The latter can therefore be arbitrarily *chosen* in such a way that the quasi-atomic orbitals become as atomic-like as possible.

By collecting the basis orbitals on each atom, the wave function Ψ is cast in the form

$$\Psi = \frac{(\psi_A + \psi_B)}{\sqrt{(2+2S)}} \qquad S = \langle \psi_A | \psi_B \rangle = 0.588742 \tag{1.10}$$

$$\psi_x = a\mathbf{s}_x + b\mathbf{p}_{x,} \quad \mathbf{s} = \sum (14\text{s}), \quad \mathbf{p} = \sum (6\text{p}, 3\text{d}, 2\text{f}, 1\text{g}) \tag{1.11}$$

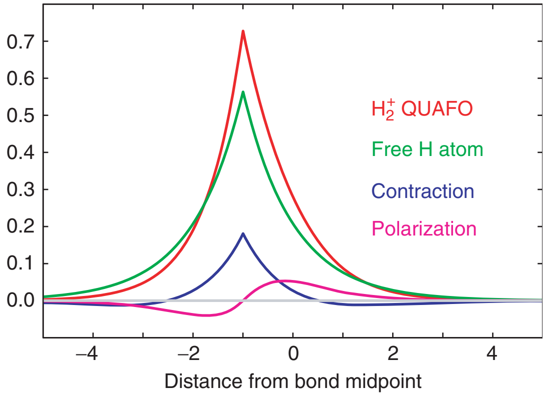

Figure 1.3 Resolution of the quasi-atomic orbital (QUAFO) on the left atom in $H_2{}^+$ as a sum of contributions from the atomic 1s orbital, the spherical deformation and the angular deformation at the equilibrium distance (see Section 1.4.1).

where ψ, $\mathbf{s}$, and $\mathbf{p}$ are normalized. The molecular FORS space is then formed by this occupied bonding orbital Ψ and by choosing the unoccupied antibonding orbital to be

$$\Psi^* = \frac{(\psi_\mathrm{A} - \psi_\mathrm{B})}{\sqrt{2 - 2S}} \tag{1.12}$$

Application of the SVD to the rectangular overlap matrix between these two molecular FORS orbitals and the set of all atomic basis orbitals on atom A manifestly yields the orbital ψ_A as the quasi-atomic orbital on A: the QUAFO orbital is in fact identical with the PAAO orbital. The same holds for atom B. Thus ψ_A and ψ_B are directly the quasi-atomic orbitals in this case.

Figure 1.3 exhibits the resolution (Eq. (1.11)) of the quasi-atomic orbital ψ_A on the left atom in terms of its components along the internuclear axis, for the equilibrium distance. In this figure the spherical component $\mathbf{s}$ has been further resolved in terms of the free-atom 1s orbital and the spherical deformation [s – (1s)]. The curves display the total respective contributions, *including coefficients*, so that adding the spherical deformation (blue) and the angular deformation (purple) to the free-atom 1s orbital (green) will yield the quasi-atomic orbital (red). At this distance, the spherical deformation is manifestly a contraction and the angular deformation represents a polarization.

The total relative contributions of the spherical and the angular deformations to the quasi-atomic orbital, i.e., their integrated contributions to the normalization integral, as well as their variations with the internuclear distance R are shown in Figure 1.4. The polarization deformation contributes less than 2% over the whole range, but its contribution extends to fairly large internuclear distances. The spherical deformation effectively vanishes beyond 4 Bohr, but strongly increases for shorter distance, being ~4% at the equilibrium distance.

Regarding the *normalized spherical* component $\mathbf{s}$ in Eq. (1.11), the following observation is important:

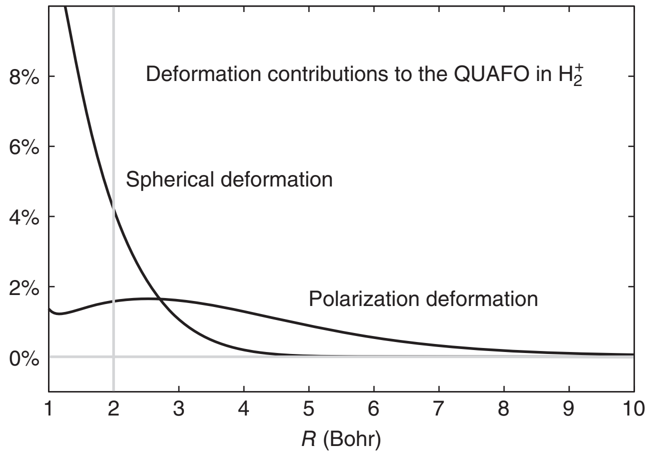

Figure 1.4 Variation of the spherical and angular deformations of the quasi-atomic orbital in $H_2{}^+$ with the internuclear distance. The gray vertical line indicates the equilibrium distance.

> The spherical component of the quasi-atomic orbital is near-identical with a scaled hydrogen-like orbital 1s* of the type formulated in Eq. (1.5).

This agreement is demonstrated in Figure 1.5 where Figure 1.5b displays the overlap integral $\langle \mathbf{s}|1s^*\rangle$ as a function of the internuclear distance R. Figure 1.5a displays the orbital exponent value ζ^* of the 1s* orbital that corresponds to the quasi-atomic orbital at each internuclear distance. This exponent was obtained by

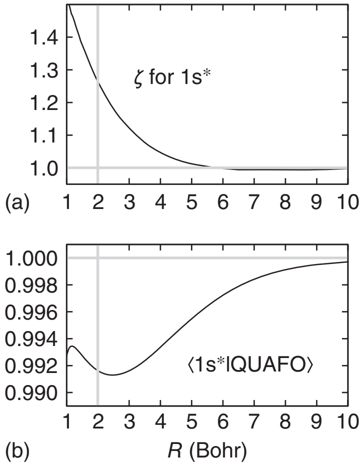

Figure 1.5 Characteristics of the exponential approximation 1s* to the spherical part of the quasi-atomic orbital (QUAFO) in $H_2{}^+$ at various internuclear distances. (a) Orbital exponent of 1s*. (b) Overlap integral between the 1s* orbital and the QUAFO. The gray vertical line indicates the equilibrium distance.

maximizing, at each internuclear distance, the overlap integral $\langle \mathbf{s}|1s^*\rangle$ with respect to the orbital exponent ζ^* in the 1s* orbital. Whereas, in the region $R > \sim 6$ Bohr, the 1s* orbital is seen to be very slightly *expanded* ($\zeta^* < 1$) with respect to the hydrogen 1s orbital ($\zeta = 1$),

> the 1s* orbital becomes considerably contracted ($\zeta^* > 1$) in the region for $R < \sim 4.5$ Bohr. At the equilibrium its orbital exponent is $\zeta^* = 1.264$.

Combining the data of Figures 1.4 and 1.5, one sees that the projection of the quasi-atomic orbital ψ_x on the scaled $1s_x$* orbital, that is, $[a \times \langle \mathbf{s}|1s^*\rangle]$, is always larger than 0.982.

1.4.2
Molecular Electron Density and Gradient Density as Sums of Intra-atomic and Interatomic Contributions

The potential energy is determined by the electron density. The kinetic energy is determined by the gradient density (see Eq. (1.4)). Therefore, both densities have to be resolved in terms of intra-atomic and interatomic contributions.

1.4.2.1 Resolution of the Molecular Density

In classical electrostatics an approximate charge distribution covering the two atoms would be a superposition of *quasi-atomic densities*, for example,

$$\rho_{\mathrm{qa}} = \frac{1}{2}(\psi_{\mathrm{A}}^2 + \psi_{\mathrm{B}}^2) \tag{1.13}$$

In quantum mechanics, by contrast, the quasi-atomic *wave amplitudes* are superposed, as expressed in Eq. (1.10), so that the molecular density $\rho = \Psi^2$ differs from the *quasi-atomic* density ρ_{qa} of Eq. (1.13) as follows:

$$\Psi^2 = \rho = \rho_{\mathrm{qa}} + \rho_{\mathrm{I}}, \quad \rho_{\mathrm{I}} = \rho - \rho_{\mathrm{qa}} = \frac{\mathcal{I}_{\mathrm{AB}}}{(2+2S)} \tag{1.14}$$

where

$$\mathcal{I}_{\mathrm{AB}} = 2\psi_{\mathrm{A}}\psi_{\mathrm{B}} - S(\psi_{\mathrm{A}}^2 + \psi_{\mathrm{B}}^2) \tag{1.14a}$$

The *bond order* $(2+2S)^{-1}$ has the value 0.314714 at the equilibrium distance. In ρ, the two atomic amplitudes are summed before they are squared whereas, in ρ_{qa}, they are squared before they are summed. The difference ρ_{I} represents therefore the *interference density*, that is, the interference part of the total density ρ. The term $\mathcal{I}_{\mathrm{AB}}$ represents the *interference of the quasi-atomic orbitals*.

The integrals over ρ and ρ_{qa} are both = 1. Hence, the integral over ρ_{I} vanishes, which implies that the interference density ρ_{I} represents a *charge shift* in real space. In fact, the interference density *represents the quantification of the often qualitatively invoked "accumulation of electronic charge in the bond."* This property is exhibited in panels of Figure 1.6a–c, which display the contour plots of ρ_{I} in a plane containing the internuclear axis *at the equilibrium distance*. With a view to the subsequent discussion, plots of ρ_{I} are shown not only using the exact orbitals ψ_{A}, ψ_{B} but also

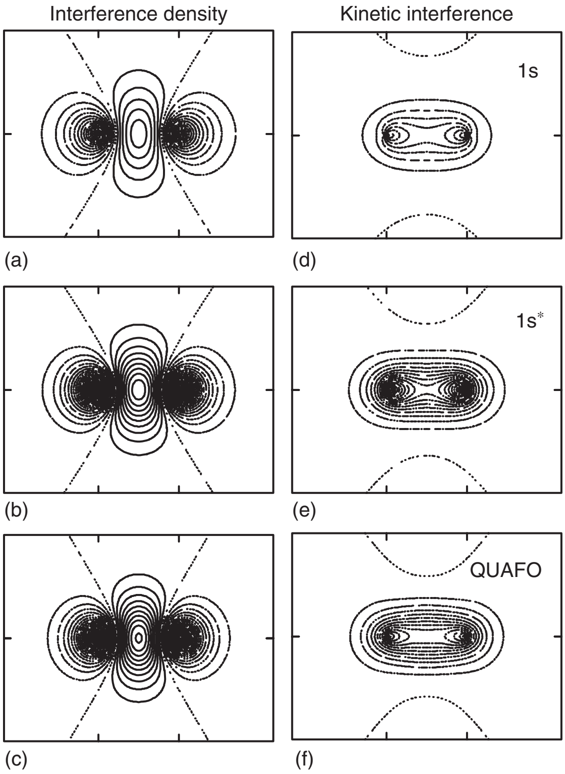

Figure 1.6 Interatomic interference in H_2^+ at the equilibrium distance. Left column of panels: interference *densities* ρ_I = charge accumulation in the bond of H_2^+. Right column of panels: kinetic interference densities = gradient attenuation. First row of panels: interference between the atomic 1s ground state orbitals. Second row of panels: interference between the scaled exponential 1s* approximations to the QUAFOs (see Figure 1.5). Third row of panels: interference between the quasi-atomic orbitals (QUAFOs) of the actual wave function of H_2^+. Contour increments: left panels: 0.002 e Bohr^{-3}; right panels: 5 millihartree Bohr^{-3}. Solid lines = positive contours. Dashed lines = negative contours. Dotted lines = zero contours.

using the hydrogen 1s orbitals as well as using the scaled 1s* orbitals discussed at the end of the preceding Section 1.4.1. Note should be made of the fact that

> for all quasi-atomic orbital choices, even when polarization is included, the charge that is accumulated in the bond is taken away from regions near the nuclei.

This aspect of the charge accumulation in the bond is often overlooked.

1.4.2.2 Resolution of the Molecular Gradient Density

The gradient density $(\nabla\psi)^2$ can be resolved in a similar way as the density ψ^2, that is, in terms of the average of the atomic gradient densities and the difference between this term and the molecular gradient density, that is,

$$(\nabla\Psi)^2 = \frac{[(\nabla\psi_A)^2 + (\nabla\psi_B)^2]}{2} + \left\{(\nabla\Psi)^2 - \frac{[(\nabla\psi_A)^2 + (\nabla\psi_B)^2]}{2}\right\} \tag{1.15}$$

In analogy to the interference density ρ_I, the difference term in the curly brackets on the right hand side can be considered as the *gradient interference density*. Panels in Figure 1.6d–f exhibit contours of this gradient interference densities at the equilibrium distance. *All of them are negative*, showing that the superposition of the quasi-atomic orbitals attenuates the gradient of Ψ everywhere, when compared to the average of the quasi-atomic gradient densities. Along the internuclear axis, this attenuation is manifest by comparing the plots of Ψ^2 and $({\psi_A}^2 + {\psi_B}^2)/2$, as shown, for example, in Figure 9 of Ref. [13a].

The interference density as well as the gradient interference density result from the spread of the *orbital amplitude* from one atom to two atoms. Both are thus consequences and exhibit different aspects of the *orbital delocalization*. This inference will be confirmed by the energy analyses in Sections 1.4.5.2 (last paragraph) and 1.4.5.4 (first paragraph).

A difference in interpretation between Eqs. (1.15) and (1.14) is the following. Although both equations furnish resolutions in terms of intra-atomic contributions and interference contributions, only the sum of the intra-atomic *density* contributions in Eq. (1.14) can be considered as "quasi-classical." *This cannot be claimed for the intra-atomic gradient densities* because, as discussed in Section 1.2.1, the treatment of the kinetic energy in quantum mechanics is fundamentally different from that in classical mechanics.

1.4.3
Dependence of Delocalization and Interference on the Size of the Quasi-Atomic Orbitals

It turns out that a rather important role in the process of bonding is played by the *dependence* of the magnitude of interference on the *size of the quasi-atomic orbitals relative to the distance R between the nuclei*. This dependence is not trivially obvious.

From the definition in Eq. (1.14) one sees immediately that the interference density vanishes for $R = 0$ as well as for $R = \infty$. In between these two limiting cases, it must therefore wax and wane. On the other hand, comparing the interference contours on Figure 1.6a, obtained for the hydrogen 1s orbitals, with those on Figure 1.6b, obtained using the contracted 1s* orbitals, one notes that, at the equilibrium distance, *the accumulation of charge in the bond is stronger for the contracted 1s* orbitals than for the uncontracted 1s orbitals. Similarly, the kinetic interference density of 1s* in panel e of that figure is stronger in the bond than that of 1s in panel d. This correlation is, at first sight, surprizing since the overlap integral decreases with contraction.* The observations are put in perspective by the following explicit analysis for the case that the quasi-atomic orbitals are approximated by the scaled 1s-type orbital $1s_\zeta$ defined in Eq. (1.5).

1.4.3.1 **Charge Accumulation at the Bond Midpoint**

The contours in Figure 1.6a–c suggest that the maximum of the charge accumulation in the bond, which occurs at the bond midpoint, offers a rough measure of the magnitude of the interference ρ_I. By virtue of the definition in Eq. (1.14), this value is given by

$$\rho_{\mathrm{I,mid}}(\psi_\mathrm{A}) = \frac{\Psi^2 - (\psi_\mathrm{A}^2 + \psi_\mathrm{B}^2)}{2} = \psi_\mathrm{A}^2 \times \frac{(1-S)}{(1+S)}, \quad S = \langle \psi_\mathrm{A} | \psi_\mathrm{B} \rangle \tag{1.16}$$

where ${\psi_\mathrm{A}}^2$ is taken at the bond midpoint. If the scaled $1\mathrm{s}_\zeta$ orbital of Eq. (1.5) is used as an approximation to the quasi-atomic orbital ψ_A, the Eq. (1.16) becomes

$$\rho_{\mathrm{I,mid}}(1s_\zeta) = \left(\frac{1}{\pi R^3}\right)\left\{\left[\frac{(1-S)}{(1+S)}\right]\sigma^3 \exp(-\sigma)\right\} \tag{1.17}$$

where

$$S = \left(1 + \sigma + \frac{\sigma^2}{3}\right) \times \exp(-\sigma), \quad \sigma = \zeta R \tag{1.18}$$

Relevant in the present context is the dependence of $\rho_{\mathrm{I,mid}}$ on the orbital size *at any given internuclear distance*. This dependence is given by the expression in the curly brackets {} in Eq. (1.17), which is a function of $\sigma = \zeta R = R/\alpha$ = the inverse ratio of the orbital size to the internuclear distance. This dependence on σ is displayed in Figure 1.7a, which is a plot of $\rho_{\mathrm{I,mid}}$ versus σ, where the equilbrium value has been arbitrarily chosen for the factor R^{-3} *in front of the curly bracket*. Since the maximum of the curve occurs for $\sigma = \zeta R = 4.01$, the criterion suggests that the maximal charge accumulation in the bond is obtained for a value ${\zeta_\mathrm{m}}' > 1$ when $R < 4.01$ Bohr, but for a value ${\zeta_\mathrm{m}}' < 1$ when $R > 4.01$ Bohr. With reference to the hydrogen 1s orbital (i.e., $\zeta = 1$), *maximal charge accumulation in the bond, according to this criterion, is therefore obtained by orbital contraction when $R < {\sim}4$ Bohr, and by orbital expansion when $R > {\sim}4$ Bohr*.

1.4.3.2 **Total Charge Accumulation in the Bond**

Alternatively, an *overall measure* of the charge accumulation in the bond can be obtained by calculating the amount of charge that interference in fact shifts from the atomic regions into the bond region, that is, from the regions with negative contours into the region with positive contours of ρ_I in Figure 1.6. These three regions are separated by the two-sheet hyperboloid on which ρ_I vanishes. For the quasi-atomic orbitals $1\mathrm{s}_\zeta$, it is given by

$$\frac{(R_\mathrm{A} - R_\mathrm{B})}{R} = \frac{\pm a(\sigma)}{\sigma}, \quad a(\sigma) = \operatorname{arccosh}\left[\frac{1}{S(\sigma)}\right] = \ln\left\{\frac{\left[1 + \left(1 - S^2\right)^{\frac{1}{2}}\right]}{S}\right\} \tag{1.19}$$

Integration of ρ_I over the central region between the two hyperboloid sheets yields the total charge Q_I that is actually moved from the atomic regions into the bond region. It is found to be

$$Q_\mathrm{I}(1s_\zeta) = \left[\left(2\sigma + \sigma^2\right)\left(a - \left(1 - S^2\right)^{\frac{1}{2}}\right) + a^2(1 - S^2)^{\frac{1}{2}} - \frac{a^3}{3}\right]\left[\frac{\exp(-\sigma)}{2\sigma(1+S)}\right] \tag{1.20}$$

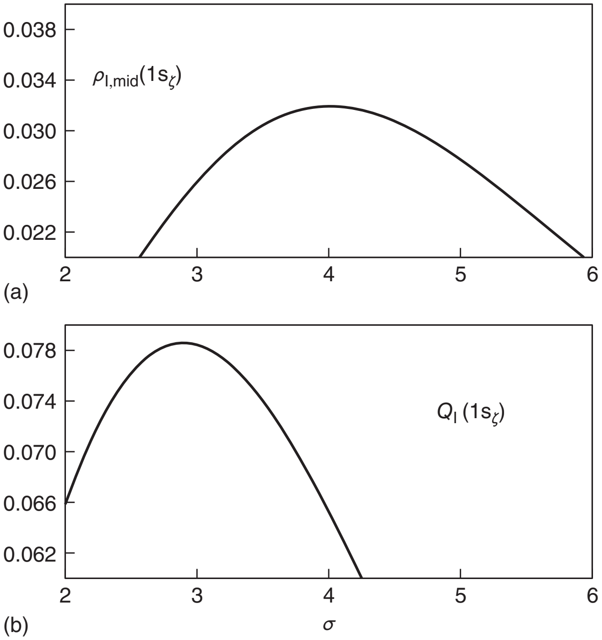

Figure 1.7 Variation of the strength of the interference density ρ_I between scaled $1s_\zeta$ orbitals (of Eq. (1.5)) with the orbital size $\alpha = 1/\zeta$ relative to the internuclear distance R. Abscissa: $\sigma = \zeta R = R/\alpha$. Ordinate of (a): value of ρ_I at the bond mid point (Eq. (1.17)). Ordinate of (b): integrated charge accumulation into the bond (Eq. (1.20)). For details, see text.

where σ, $S(\sigma)$, and $a(\sigma)$ are defined in Eqs. (1.18) and (1.19). Figure 1.7b displays the variation of the total charge accumulation $Q_I(\sigma)$ as a function of σ. Its maximal value occurs for $\sigma = 2.90$ Bohr. According to this criterion, interference is enhanced by contraction when $R < \sim 2.9$ Bohr and by expansion when $R > \sim 2.9$ Bohr.

1.4.3.3 **Origin of the Relation between Interference and Quasi-Atomic Orbital Contraction/Expansion**

The foregoing assessments show that, at shorter internuclear distances, interference is enhanced by contraction of the hydrogen AOs whereas, at larger internuclear distances, it is enhanced by expansion of these orbitals. The switchover occurs somewhere in the region around twice the equilibrium distance. A remarkable implication is that, whereas interference increases with increasing quasi-atomic orbital overlap at larger distances, *interference increases* with *decreasing overlap by contraction* at shorter distances, as noted earlier.

This consequential attribute of interference can be traced back to the following property of interfering AOs. Consider a scaled hydrogen orbital $\phi(r, \zeta) = 1s_\zeta$, as defined in Eq. (1.5). Because normalization is preserved, *the scaled orbital* $1s_\zeta = \phi(r, \zeta)$ *and the unscaled orbital* $1s = \phi(r, \zeta = 1)$ *cross over at some distance* r^* *from the* *origin*. Manifestly, when $\zeta > 1$, then $\phi(r, \zeta)$ is contracted relative to 1s and one has

$$\phi(r,\zeta) > 1\text{s} \quad \text{for } r < r^*, \quad \phi(r,\zeta) < 1\text{s} \quad \text{for } r > r^* \tag{1.21a}$$

whereas, when $\zeta < 1$, then $\phi(r, \zeta)$ is expanded relative to 1s and one has

$$\phi(r,\zeta) < 1\text{s} \quad \text{for } r < r^*, \quad \phi(r,\zeta) > 1\text{s} \quad \text{for } r > r^* \tag{1.21b}$$

Moreover, one deduces from the equality $\phi(r^*, \zeta) = 1\text{s} = \phi(r^*, 1)$ at the crossover radius r^* that the value of this radius depends on ζ according to

$$r^*(\zeta) = \left[\frac{(\log \zeta)}{(\zeta - 1)}\right] \times 1.5\,\text{bohr} \tag{1.22a}$$

and, since $r^*(\zeta)$ is a monotonic function, there exists a scaled orbital $\phi(r, \zeta)$ with a certain $\zeta = \zeta(r^*)$ for any chosen crossover point r^*. It follows from Eq. (1.22a) that

$$r^*(\zeta) < 1.5 \quad \text{for } \zeta > 1, \quad r^*(\zeta) = 1.5 \quad \text{for } \zeta = 1, \quad r^*(\zeta) > 1.5 \quad \text{for } \zeta < 1 \tag{1.22b}$$

and, conversely, that

$$\zeta(r^*) > 1 \quad \text{when } r^* < 1.5, \quad \zeta(r^*) < 1 \quad \text{when } r^* > 1.5 \tag{1.22c}$$

Consider now two scaled 1s orbitals placed at an internuclear distance $2R$ of less than 3 Bohr so that the bond midpoint is at a distance $R < 1.5$ Bohr from each nucleus. For each value of r^* in the range $R < r^* < 1.5$ Bohr, there then exists a scaled orbital $\phi(r, \zeta)$ on each nucleus that (i) has $\zeta = \zeta(r^*) > 1$, i.e., that is *contracted* relative to the respective uncontracted 1s orbital (see Eq. (1.22c), left), and (ii) is *larger* than the respective 1s orbital, that is $\phi(r, \zeta) > 1\text{s}$, for all distance $r \leq R$ from that nucleus (see Eq. (1.21a), left). This is so, in particular at the bond midpoint, where $r = R$. Therefore, according to Eq. (1.16), *the charge accumulation of the superposition of the two contracted orbitals at the bond midpoint is larger than that of the superposition of two uncontracted orbitals*. (Note that the factor $(1 - S)/(1 + S)$ in Eq. (1.16) is also larger for the contracted orbitals, because the overlap integral between them is smaller than that for the uncontracted orbitals.) Thus, *when the two orbital centers are closer than 3 Bohr, quasi-atomic orbital contraction enhances charge accumulation in the bond and, hence, interference and delocalization between these orbitals*. It is also apparent that similar inferences can be drawn for any suitably decaying quasi-atomic orbitals [14]. This aspect of interference has not been previously noted.

As shown by an analogous analysis, the enhancement increasingly diminishes as the internuclear distance becomes longer than 3 Bohr and, for sufficiently large distances, charge accumulation in the bond is enhanced by orbital expansion rather than contraction.

1.4.4
Binding Energy as a Sum of Two Intra-atomic and Three Interatomic Contributions

The well-known general shapes of the kinetic and potential components of the binding energy curve exhibit very different behaviors at larger and shorter internuclear distances. These shapes suggest that the binding energy is the result of several contributions with different distance dependencies. In fact, five contributions with distinct conceptual physical meanings can be identified. They are formulated in the present section. In the next section their quantitative properties are discussed and in the subsequent section their synergism is traced.

Substitution of the density decomposition (Eq. (1.14)) into the potential energy integral of $H_2{}^+$ yields the following resolution of the potential energy of $H_2{}^+$ in terms of three contributions:

$$\mathbf{V}(\Psi) = \int \mathrm{d}x \left(-\frac{1}{r_\mathrm{A}} - \frac{1}{r_\mathrm{B}}\right)\rho + \frac{1}{R} = \mathbf{V}_\mathrm{a} + \mathbf{V}_\mathrm{qc} + \mathbf{V}_\mathrm{I} \tag{1.23}$$

where the individual terms have the following definitions and physical meanings

$$\begin{aligned}\mathbf{V}_\mathrm{a} &= \frac{\left\{-\int \mathrm{d}x\, \psi_\mathrm{A}^2/r_\mathrm{A} - \int \mathrm{d}x\, \psi_\mathrm{B}^2/r_\mathrm{B}\right\}}{2}\\ &= \text{the } \textit{intra-atomic} \text{ potential energy of the quasi-atomic orbitals}\end{aligned} \tag{1.24}$$

$$\begin{aligned}\mathbf{V}_\mathrm{qc} &= \frac{\left\{-\int \mathrm{d}x\, \psi_\mathrm{A}^2/r_\mathrm{B} - \int \mathrm{d}x\, \psi_\mathrm{B}^2/r_\mathrm{A}\right\}}{2} + \frac{1}{R}\\ &= \text{the } \textit{quasi-classical coulombic interatomic} \text{ potential energy}\end{aligned} \tag{1.25}$$

$$\begin{aligned}\mathbf{V}_\mathrm{I} &= \int \mathrm{d}x \left(-\frac{1}{r_\mathrm{A}} - \frac{1}{r_\mathrm{B}}\right)\rho_\mathrm{I}\\ &= [2(1+S)]^{-1}\int \mathrm{d}x \left(-\frac{1}{r_\mathrm{A}} - \frac{1}{r_\mathrm{B}}\right)\mathscr{I}_\mathrm{AB}\\ &= \text{the } \textit{inter-atomic} \text{ potential energy due to the charge accumulation}\\ &\quad\ \text{in the bond}\\ &= \text{the potential } \textit{interference} \text{ energy. } [\mathscr{I}_\mathrm{AB} \text{was defined in Eq. (1.14a)}]\end{aligned} \tag{1.26}$$

The potential part of the *binding energy*, that is,

$$\mathbf{V}_\mathrm{binding} = \mathbf{V}(\Psi) - \mathbf{V}_\mathrm{H} \quad \text{with } \mathbf{V}_\mathrm{H} = -\int \mathrm{d}x \frac{(1\mathrm{s}_\mathrm{A})^2}{r_\mathrm{A}} = -1\,\text{hartree} \tag{1.27}$$

is therefore the sum of an intra-atomic and an interatomic contribution:

$$\mathbf{V}_\mathrm{binding} = \mathbf{V}_\mathrm{intra} + \mathbf{V}_\mathrm{inter} \tag{1.28}$$

where

$$\mathbf{V}_\mathrm{intra} = \mathbf{V}_\mathrm{a} - \mathbf{V}_\mathrm{H}, \quad \mathbf{V}_\mathrm{inter} = \mathbf{V}_\mathrm{qc} + \mathbf{V}_\mathrm{I} \tag{1.29}$$

The analogous resolution of the kinetic energy is simpler, viz,

$$\mathbf{T}(\Psi) = \frac{1}{2}\int \mathrm{d}x\,(\nabla\Psi)^2 = \mathbf{T}_{\mathrm{a}} + \mathbf{T}_{\mathrm{I}} \tag{1.30}$$

where

$$\begin{aligned}\mathbf{T}_{\mathrm{a}} &= \frac{\left\{\frac{1}{2}\int \mathrm{d}x\,(\nabla\psi_{\mathrm{A}})^2 + \frac{1}{2}\int \mathrm{d}x\,(\nabla\psi_{\mathrm{B}})^2\right\}}{2}\\ &= \text{the } \textit{intra-atomic} \text{ kinetic energies of the quasi-atomic orbitals}\end{aligned} \tag{1.31}$$

$$\begin{aligned}\mathbf{T}_{\mathrm{I}} &= \frac{1}{2}\int \mathrm{d}x \left\{(\nabla\Psi)^2 - \frac{[(\nabla\psi_{\mathrm{A}})^2 + (\nabla\psi_{\mathrm{B}})^2]}{2}\right\}\\ &= \frac{1}{2}\int \mathrm{d}x\,\frac{\{2(\nabla\psi_{\mathrm{A}})\cdot(\nabla\psi_{\mathrm{B}}) - [(\nabla\psi_{\mathrm{A}})^2 + (\nabla\psi_{\mathrm{B}})^2]\}}{2(1+S)}\\ &= \text{the } \textit{interatomic} \text{ kinetic } \textit{interference} \text{ energy}\\ &= \text{the } \textit{interatomic} \text{ kinetic energy resulting from the orbital delocalization}\end{aligned} \tag{1.32}$$

The kinetic part of the binding energy, that is,

$$\mathbf{T}_{\mathrm{binding}} = \mathbf{T}(\Psi) - \mathbf{T}_{\mathrm{H}} \quad \text{with} \quad \mathbf{T}_{\mathrm{H}} = \frac{1}{2}\int \mathrm{d}x\,\frac{(\nabla 1s_{\mathrm{A}})^2}{r_{\mathrm{A}}} = 0.5\,\text{hartree} \tag{1.33}$$

is thus also the sum of an intra-atomic and an interatomic contribution:

$$\mathbf{T}_{\mathrm{binding}} = \mathbf{T}_{\mathrm{intra}} + \mathbf{T}_{\mathrm{inter}} \tag{1.34}$$

with

$$\mathbf{T}_{\mathrm{intra}} = \mathbf{T}_{\mathrm{a}} - \mathbf{T}_{\mathrm{H}}, \quad \mathbf{T}_{\mathrm{inter}} = \mathbf{T}_{\mathrm{I}} \tag{1.35}$$

By virtue of Eq. (1.4) each kinetic term is a sum of an x, y, and z component, where the z-direction is conventionally taken along the internuclear axis. It should again be emphasized that the definitions Eqs. (1.30)–(1.33) of the kinetic terms could all have been equally well written in terms of the Laplacian expression of the kinetic energy. As mentioned earlier, the gradient form is preferred in order that positive kinetic energy terms appear with positive signs in front of them.

Combining the preceding resolutions yields the following decomposition of the binding energy in terms of intra-atomic and interatomic contributions:

$$\mathbf{E}_{\mathrm{Binding}} = \mathbf{E}(\Psi) - \mathbf{E}_{\mathrm{H}} = \mathbf{E}_{\mathrm{intra}} + \mathbf{E}_{\mathrm{inter}} \tag{1.36}$$

$$\mathbf{E}_{\mathrm{intra}} = \mathbf{E}_{\mathrm{a}} - \mathbf{E}_{\mathrm{H}} = \mathbf{T}_{\mathrm{intra}} + \mathbf{V}_{\mathrm{intra}} \tag{1.37a}$$

$$\mathbf{T}_{\mathrm{intra}} = (\mathbf{T}_{\mathrm{a}} - 0.5\text{ hartree}), \qquad \mathbf{V}_{\mathrm{intra}} = (\mathbf{V}_{\mathrm{a}} + 1.0\text{ hartree}) \tag{1.37b}$$

$$\mathbf{E}_{\mathrm{inter}} = \mathbf{E}_{\mathrm{I}} + \mathbf{V}_{\mathrm{qc}} = \mathbf{T}_{\mathrm{inter}} + \mathbf{V}_{\mathrm{inter}}, \qquad \mathbf{E}_{\mathrm{I}} = \mathbf{T}_{\mathrm{I}} + \mathbf{V}_{\mathrm{I}} \tag{1.38a}$$

$$\mathbf{T}_{\text{inter}} = \boxed{\mathbf{T}_{\text{I}}} \qquad \mathbf{V}_{\text{inter}} = \boxed{\mathbf{V}_{\text{I}} + \mathbf{V}_{\text{qc}}} \tag{1.38b}$$

The binding energy has thus the five basic conceptual physical components shaded in yellow in Eqs. (1.37)–(1.38), viz: the intra-atomic energy changes $\mathbf{T}_{\text{intra}}$ and $\mathbf{V}_{\text{intra}}$, which are due to the deformation from the free atom to the quasi-atom in the molecule, and the interatomic energy changes $\mathbf{V}_{\text{qc}}$, $\mathbf{V}_{\text{I}}$, and $\mathbf{T}_{\text{I}}$, which embody the quasi-classical interactions and the interference interactions that are generated by delocalization between the quasi-atomic orbitals on the two centers.

1.4.5
Quantitative Characteristics of the Five Energy Contributions

By virtue of the physical meanings of the five energy contributions, certain general features of their quantitative values can be identified that are relevant for understanding the behavior of the kinetic, potential, and total energy curves.

1.4.5.1 Intra-atomic Deformation Energy: $\mathbf{E}_{\text{intra}} = \mathbf{T}_{\text{intra}} + \mathbf{V}_{\text{intra}}$

The intra-atomic deformation energy $\mathbf{E}_{\text{intra}}$ of (Eq. (1.37)) is the energy deviation from the free-atom minimum. By virtue of the *atomic* variation principle, *it is necessarily positive*, that is, it has an antibonding effect. In particular, as discussed in detail in Section 1.2.2, upon quasi-atomic orbital *contraction*, $\mathbf{T}_{\text{intra}}$ will become more positive and $\mathbf{V}_{\text{intra}}$ will become more negative, with $\mathbf{T}_{\text{intra}}$ prevailing over $\mathbf{V}_{\text{intra}}$.

1.4.5.2 Quasi-Classical Interaction between the Atoms: $\mathbf{V}_{\text{qc}}$

By virtue of the molecular symmetry, the quasi-classical energy of Eq. (1.25) can also be written as

$$\mathbf{V}_{\text{qc}} = -\int \mathrm{d}x \frac{\psi_{\text{A}}^2}{r_{\text{B}}} + \frac{1}{R} \tag{1.39}$$

It is thus the potential energy of a neutral hydrogen atom at A, with a *fixed* density $\psi_{\text{A}}{}^2$, in the field of a proton B at a distance R from A.

If $\psi_{\text{A}}{}^2$ is spherically symmetric then, as Newton first showed [22], the first term on the right hand side of Eq. (1.39) equals $\{R^{-1}[-\int \mathrm{d}x\, \psi_{\text{A}}{}^2]\}$ where the integration goes over the sphere with radius R around A. Since this sphere encompasses less than the whole of $\psi_{\text{A}}{}^2$, the integral $\int \mathrm{d}x\, \psi_{\text{A}}{}^2$ is <1 and, hence, $\mathbf{V}_{\text{qc}}$ becomes positive, that is, *antibonding*. If the spherical quasi-atomic orbital is *contracted*, then the integral $[-\int \mathrm{d}x\, \psi_{\text{A}}{}^2]$ is closer to 1 and increases the shielding of nucleus A so that $\mathbf{V}_{\text{qc}}$ will become *less repulsive*. Expansion of the quasi-atomic orbital will have the opposite effect.

For $\mathbf{V}_{\text{qc}}$ to be attractive, the orbital ψ_{A} has to become sufficiently polarized toward nucleus B.

It may also be noted that the form of Eq. (1.39) for $\mathbf{V}_{\text{qc}}$ implies that the effect of orbital delocalization on the potential energy is entirely contained in the interference energy $\mathbf{V}_{\text{I}}$. The interference density is therefore an expression of delocalization in agreement with the discussion at the end of Section 1.4.2.2.

1.4.5.3 Potential Interference Energy: $\mathbf{V}_\mathrm{I}$

According to the analysis in Section 1.4.2.1, the interference density ρ_I shifts charge from near the nuclei toward the bond center, where the potential $(-1/r_\mathrm{A} - 1/r_\mathrm{B})$ is less negative than near the nuclei. Therefore, *the potential interference energy of Eq. (*1.26*) is always positive, that is, antibonding*.

The rather popular hand waving conjecture that charge accumulation through overlap in the bonds of H_2 and H_2^+ *lowers* the potential energy is patently wrong.

1.4.5.4 Kinetic Interference Energy: $\mathbf{T}_\mathrm{I}$

By virtue of the molecular symmetry, the kinetic interference energy of Eq. (1.32) can be written

$$\mathbf{T}_\mathrm{I} = \frac{1}{2}\int \mathrm{d}x\,(\nabla\Psi)^2 - \frac{1}{2}\int \mathrm{d}x\,(\nabla\psi_\mathrm{A})^2 \tag{1.40}$$

where the wave function $\Psi \sim (\psi_\mathrm{A} + \psi_\mathrm{B})$ is manifestly more delocalized than the orbital ψ_A. According to the basic insights of Section 1.2.1, the first term in this equation is therefore expected to have a lower kinetic energy than the second term so that *the kinetic interference energy will be negative, that is, bonding*. This expectation is confirmed by the contours on panels of Figure 1.6d–f in Section 1.4.2.2, which show that the integrand in Eq. (1.32) is negative everywhere. The conjunction of Eq. (1.40) and Figure 1.6 also confirms the inference at the end of Section 1.4.2.2 that the gradient interference density is an expression of delocalization.

Since superposing the AOs attenuates the derivative *along* the bond axis most strongly, the component in this direction is found to contribute 2/3 of the negative value of $\mathbf{T}_\mathrm{I}$ at the equilibrium distance [13].

1.4.5.5 Interference Energies and Quasi-Atomic Orbital Contraction and Expansion

According to the discussions in Sections 1.4.2.2 and 1.4.5.2, charge accumulation in the bond goes hand in hand with orbital delocalization. The analysis in Section 1.4.3 had shown that, for $R < 3$–4 Bohr, charge accumulation in the bond as well as delocalization increase when the quasi-atomic orbitals *contract* (with respect to the free-atom 1s orbitals) whereas, for $R > 3$–4 Bohr, charge accumulation in the bond and delocalization increase when the quasi-atomic orbitals *expand*. These changes with orbital shrinking and swelling lead to the following changes in the kinetic and potential interference energies.

According to the discussion in Section 1.4.5.3, increasing the charge accumulation in the bond will make $\mathbf{V}_\mathrm{I}$ more positive (antibonding). Therefore, *quasi-atomic orbital contraction of the free-atom 1s orbitals is expected to increase the antibonding effect of the potential interference energy when $R < \sim 4$ Bohr whereas the opposite holds when $R > \sim 4$ Bohr*. This inference is confirmed by explicit calculation of $\mathbf{V}_\mathrm{I}$ for the case that the quasi-atomic orbitals are chosen to be of the scaled $1s_\zeta$ type defined in Eq. (1.5) with a variable exponent ζ. The potential interference energy is then found to be

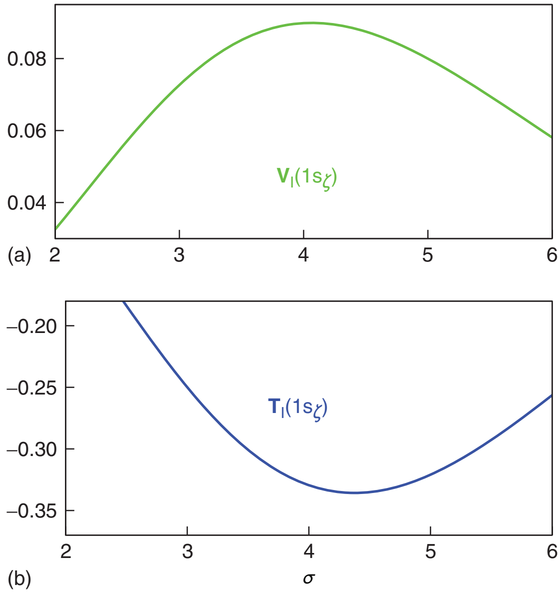

Figure 1.8 Variation of the strengths of the interference energies between scaled $1s_\zeta$ orbitals (of Eq. (1.5)) with the orbital size $\alpha = 1/\zeta$ relative to the internuclear distance R. Abscissa: $\sigma = \zeta R = R/\alpha$. (a) Potential interference energy. (b) Kinetic interference energy. For details, see text after Eq. (1.41) and (1.42).

$$\mathbf{V}_{\mathrm{I}}(1s_\zeta) = R^{-1}\left\{\frac{\left[S\left(1-\mathrm{e}^{-2\sigma}\right)-2\sigma\mathrm{e}^{-\sigma}\right](1+\sigma)}{(1+S)}\right\}, \quad \sigma = \zeta R \tag{1.41}$$

where $S(\sigma)$ is the overlap integral given in Eq. (1.18). *For fixed* R, the dependence on ζ is contained, through $\sigma = \zeta R$, in the expression in the large curly brackets $\{\}$. The dependence of this expression on σ is displayed in Figure 1.8a, which is a plot of $\mathbf{V}_{\mathrm{I}}$ versus σ where the equilibrium value has been arbitrarily chosen for the factor R^{-1} *in front of the curly bracket*. The antibonding of $\mathbf{V}_{\mathrm{I}}$ is seen to be maximal for $\zeta_{\mathrm{m}} \approx 4.07/R$. Hence, for *$R < 4.07$ Bohr, contraction (i.e., increasing ζ_{m}) will increase* the positive $\mathbf{V}_{\mathrm{I}}$ whereas, *for $R > 4.07$, expansion* will increase $\mathbf{V}_{\mathrm{I}}$.

According to the discussion in Section 1.4.5.4, the negative value of $\mathbf{T}_{\mathrm{I}}$ is due to delocalization, and therefore, increasing delocalization will make $\mathbf{T}_{\mathrm{I}}$ more negative (bonding). Quasi-atomic orbital contraction is therefore expected to enhance the negative kinetic interference energy for $R < \sim 4$ Bohr, whereas the opposite occurs for $R > \sim 4$ Bohr. This effect on the kinetic interference energy is confirmed through explicit calculation of $\mathbf{T}_{\mathrm{I}}$ by choosing as quasi-atomic orbitals the scaled 1s-type orbitals defined in Eq. (1.5) with a variable exponent ζ. The kinetic interference energy at any given internuclear distance R is then readily found to be

$$\mathbf{T}_{\mathrm{I}}(1s_\zeta) = R^{-2}\left\{\frac{\left(-\sigma^4\mathrm{e}^{-\sigma}\right)}{3(1+S)}\right\} \tag{1.42}$$

where σ and S are the same quantities as in Eq. (1.41). *For fixed R*, the dependence on ζ is contained, through $\sigma = \zeta R$, in the expression in the large curly brackets {}. The dependence of this expression on σ is displayed in Figure 1.8b, which is a plot of $\mathbf{T}_\mathrm{I}$ versus σ, where the equilibrium value has been arbitrarily chosen for the factor R^{-2} *in front of the curly bracket*. Its minimum occurs at $\zeta_\mathrm{m} \approx 4.38/R$, which identifies the quasi-atomic orbital with maximal interference energy lowering. *For $R < 4.38$ Bohr*, the value of ζ_m is larger than 1, which implies an *enhancement of the kinetic interference effect by quasi-atomic orbital contraction* with respect to the free-atom orbital with $\zeta = 1$. *For $R > 4.38$*, the value of ζ_m is smaller than 1, which implies an *enhancement of $\mathbf{T}_I$ with quasi-atomic orbital expansion*. It is also seen that the enhancement decreases with increasing internuclear distance as $(1/R^2)$.

Thus, the bonding character of the kinetic interference energy $\mathbf{T}_\mathrm{I}$, the antibonding character of the potential interference energy $\mathbf{V}_\mathrm{I}$, as well as the response of these quantities to quasi-atom orbital shrinking and swelling as a function of the internuclear distances, are all consequences of the delocalization of the electron from one nucleus to two nuclei.

1.4.6
Synergism of the Binding Energy Contributions along the Dissociation Curve

On the basis of the quantitative relations identified in the preceding section, the changes in the total binding energy can be understood by variational reasoning. The changes along the binding energy curve will be discussed with reference to the graphs in Figure 1.9, which exhibit the resolution of the binding energy in terms of the five components identified in Eqs. (1.36–1.38) as a function of the internuclear distance.

The three *columns* of panels exhibit the analyses that result from three different choices for the quasi-atomic orbitals ψ_A in Eq. (1.10). The last column corresponds to using the exact quasi-atomic orbitals discussed in Section 1.4.1. The second column corresponds to choosing the approximation obtained by omitting the polarization contributions in Eq. (1.10) and replacing the normalized spherically symmetric term **s** by the corresponding scaled 1s* orbital discussed at the end of Section 1.4.1. For the first column, the quasi-atomic orbitals are simply chosen to be the undeformed 1s orbital of the hydrogen atom. The *rows* of colored panels display from top to bottom: (i) the quasi-classical coulombic contributions, (ii) the interference contributions, (iii) the interatomic contributions (= the sum of the top two rows), (iv) the intra-atomic contributions, and (v) the total binding energy (= the sum of the preceding two rows).

1.4.6.1 First Column: Zeroth Order Approximation to ψ_A, ψ_B by the $1s_\mathrm{A}$, $1s_\mathrm{B}$ Hydrogen Atom Orbitals

The signs of all contributions in this column correspond exactly to the general quantitative predictions made in Section 1.4.5. The quasi-classical potential contribution (see Section 1.4.5.2) as well as the potential interference contribution

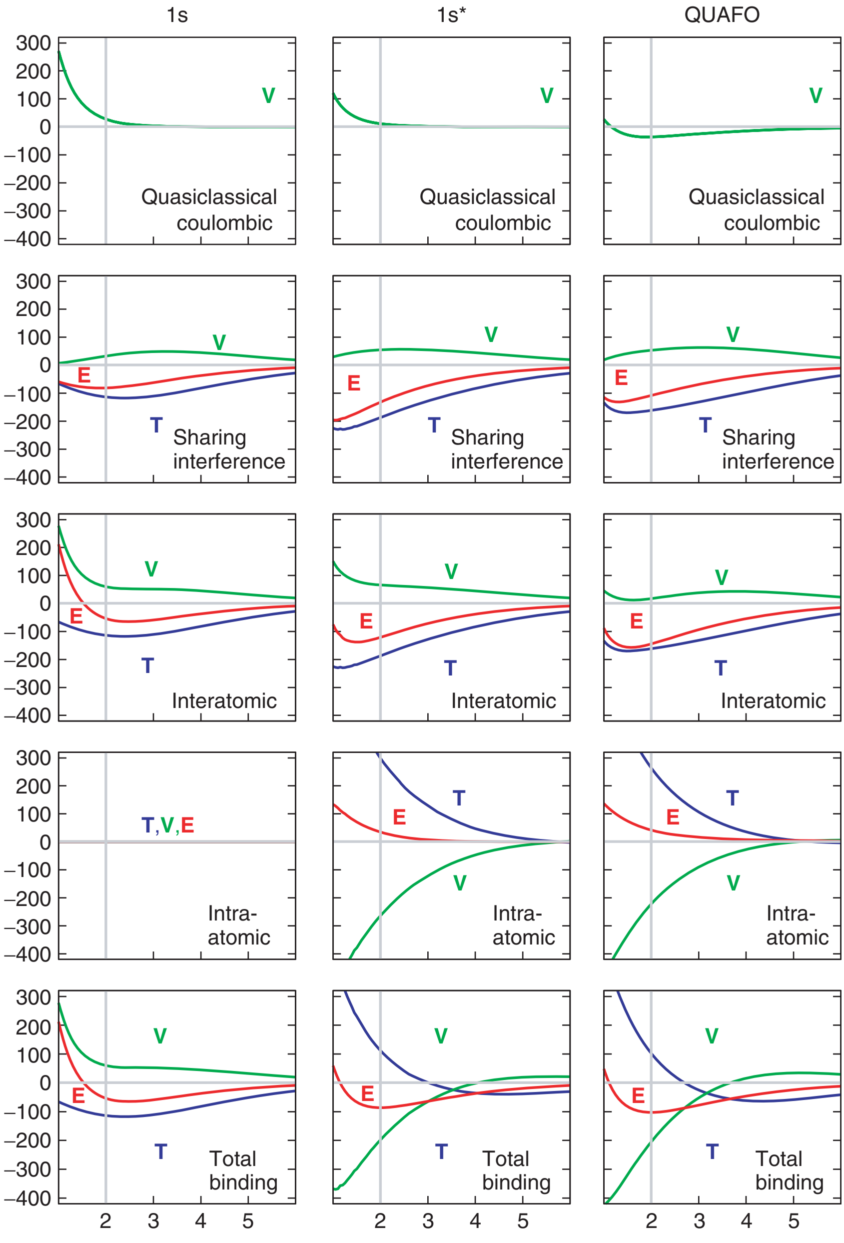

Figure 1.9 Each *column of panels* exhibits the contributions to the binding energy of H_2^+ as functions of the interatomic distance. First column: when the molecular wave function is a superposition of atomic ground state 1s orbitals. Second column: when the molecular wave function is a superposition of the scaled exponential 1s* approximations to the QUAFOs (see Figure 1.5). Third column: when the molecular wave function is a superposition of the QUAFOs, that is, for the actual wave function.

(see Section 1.4.5.3) is positive so that the *total interatomic potential energy is antibonding over the whole range. However, the negative (bonding) kinetic interference energy, which prevails at all distances, is stronger (see Section* 1.4.5.4*)*. No intra-atomic deformation energy exists, of course, in this approximation. *The total molecular binding energy is entirely due to the kinetic interference energy lowering that is a result of the delocalization.*

1.4.6.2 Second Column: Optimal Spherical Approximation to ψ_A, ψ_B by the Scaled Orbitals $1s_A$*, $1s_B$*

As noted in the last paragraph of Section 1.4.1 (see also Figure 1.5), these quasi-atomic orbitals are very slightly expanded with respect to the hydrogen 1s orbital when $R > \sim 5$ Bohr. The reason is that the expansion yields an energy lowering beyond that of the first column because the (bonding) kinetic interference energy is enhanced by expansion in this region of R (see Section 1.4.5.5) even though the (antibonding) potential interference (Section 1.4.5.5) as well as the (antibonding) quasi-classical energy (Section 1.4.5.2) is enhanced. The slight deformation of the atom is also unfavorable (Section 1.4.5.1). However, all these effects are small at large distances so that all energy contributions differ little from those in the first column.

For $R < \sim 4$ Bohr on the other hand, the 1s* orbitals increasingly contract relative to the hydrogen 1s orbital, as discussed in Section 1.4.1. The reason is that, in this region, contraction yields a marked lowering of the total energy beyond that obtained with the uncontracted orbitals shown in the first column of Figure 1.9, mainly *because of the bonding enhancement of the kinetic interference energy by increasing orbital contraction* (see discussion in Section 1.4.5.5). In addition, the *quasi-classical* energy $\mathbf{V}_{\text{qc}}$ is less repulsive than that in the first column due to enhanced shielding of the nuclei (see Section 1.4.5.2). These effects prevail over the following two changes that oppose the contraction.

First, quasi-atomic orbital contraction enhances the antibonding potential interference energy $\mathbf{V}_{\text{I}}$ beyond that of the first column (see Section 1.4.5.5). This increased antibonding in fact largely offsets the decrease in the repulsive quasi-classical energy $\mathbf{V}_{\text{qc}}$ noted in the preceding paragraph. Therefore, the total interatomic potential energy contribution $\mathbf{V}_{\text{inter}}$ is about equally antibonding as in the first column, that is, for the undeformed 1s orbitals.

Secondly, the intra-atomic energy $\mathbf{E}_{\text{intra}}$ increases as a result of the orbital deformation by virtue of the *atomic* variation principle, as was discussed in Section 1.4.5.1. It is noteworthy that this, not very large change in $\mathbf{E}_{\text{intra}}$, is the sum of a strong increase in the intra-atomic kinetic energy $\mathbf{T}_{\text{intra}}$ prevailing over an only slightly less strong decrease in the intra-atomic potential energy $\mathbf{V}_{\text{intra}}$. These changes are in fact so strong that, in this region, the kinetic contribution $\mathbf{T}_{\text{binding}}$ and the potential contribution $\mathbf{V}_{\text{binding}}$ to the total binding energy have signs that are opposite to those that they have at larger distances. This feature will be commented on further in Section 1.4.7.

1.4.6.3 Third Column: Exact Quasi-Atomic Orbitals ψ_A, ψ_B

The exact quasi-atomic orbitals differ from the 1s* orbitals by the polarization terms as shown in Eq. (1.11) and Figures 1.3 and 1.4. Because these are relatively small, the energy curves in the third column of Figure 1.9 are similar to those in the second column.

The energy lowering with respect to the second column is essentially caused by the fact that the quasi-classical energy $\mathbf{V}_{qc}$ becomes attractive as a result of the quasi-atomic orbital polarization as mentioned in Section 1.4.5.2. This energy lowering outweighs a lesser energy increase in the interference energy and in the intra-atomic energy.

The interference energy becomes slightly less bonding because polarization slightly decreases the charge accumulation in the bond. The intra-atomic energy increases because polarization is achieved by moving some of the intra-atomic electron population from an s-type orbital to a p-type orbital of the same spatial size.

1.4.6.4 Conclusion

At all internuclear distances, it is the kinetic interference interaction between the two atoms that drives the energy lowering that establishes bonding. The response of the kinetic interference interaction to swelling and shrinking of the quasi-atomic orbitals is, moreover, responsible for the peculiar variations of the kinetic energy and the potential energy with the internuclear distance.

It should be noted that, at about half the equilibrium distance, the transition to the united atom regime begins so that, for shorter internuclear distances, the physical analysis requires modification.

1.4.7

Origin of Bonding at the Equilibrium Distance

The essential factors that emerge from the detailed preceding analysis of the bond-creating quantum physical mechanism are epitomized in Table 1.1, which lists the quantitative values of the binding energy contributions *at the equilibrium distance*. The rows and columns of this table have exactly the same meanings as those described in the second paragraph of Section 1.4.6 for Figure 1.9. In light of the assessments of the preceding section, the data of Table 1.1 lead to the following conclusions on the origin of the binding energy at the equilibrium distance.

1.4.7.1 Contributions to the Binding Energy

A full understanding of the energy lowering requires that *intra*-atomic as well as *interatomic* energy changes are accounted for.

The *intra*-atomic energy changes represent deformations of the free-atom AOs to the quasi-atomic orbitals in the molecule.

The *interatomic* interactions are of two kinds: (i) quasi-classical coulombic potential energy changes due to the electrostatic interactions between the densities of the two atoms and (ii) additional energy changes that result from the quantum

Table 1.1 Binding energy analysis of H_2^+ at R_{eq} (energies in mh).

Atomic orbitals used → Interaction type ↓		Free atoms	Contracted free atoms	Quasi-atoms in molecule
Quasi-classical	V	27.6	11.3	−36.2
Interference I	T	−113.7	−187.2	−161.8
	V	32.4	54.9	53.4
	E	−81.3	−132.3	−108.4
Interatomic total	T	−113.7	−187.2	−161.8
	V	60.1	66.2	17.2
	E	−53.6	−122.0	−144.6
Intra-atomic	T	0	298.8	264.4
	V	0	−264.0	−222.4
	E	0	34.8	42.0
Total Binding	T	−113.7	111.7	102.632
	V	60.1	−197.8	−205.266
	E	−53.6	−86.2	−102.634

mechanical delocalization of the electron orbital from one atom to both atoms (“electron sharing”).

The effect of delocalization is embodied in constructive interference terms between the wave amplitudes of the AOs from the two atoms (for the antibonding orbital the interference is destructive). This constructive interference generates a shift of charge into the bond region (“charge accumulation”) as well as an attenuation of the gradient in the bond region.

In the interference energy as well as in the intra-atomic deformation energy, the kinetic contribution and the potential contribution differ in their effects on bonding.

1.4.7.2 **Energy Lowering By Electron Sharing**

The energy lowering that creates the bond is driven by the *interatomic* interactions.

This is most clearly seen when the quasi-atomic orbitals are approximated by the undeformed orbitals of the hydrogen atom so that the intra-atomic energy changes vanish, as shown in the first column of Table 1.1. In this case the energy lowering at the equilibrium distance (−53.6 mh) is caused entirely by the *kinetic* interference energy (−113.7 mh) as a result of orbital delocalization. The potential interference energy and the potential quasi-classical energies are both positive, that is, antibonding (+32.4 and +27.6 mh, respectively).

In fact, beyond thrice the equilibrium distance, the exact binding energy comes about just in this way (albeit on a smaller scale), since the quasi-atomic orbitals do not deform at these distances. However, at less than twice the equilibrium distance intra-atomic orbital deformations occur and lower the energy further.

1.4.7.3 **Energy Lowering by Quasi-Atomic Orbital Deformation**

The deformations of the hydrogen atom orbitals into the quasi-atomic orbitals unavoidably *increase the intra-atomic* energy by virtue of the *atomic* variation principle. However, the deformations *decrease the interatomic* energy contributions even more, thus yielding a decrease of the *molecular* energy.

The deformations are of two kinds: spherical contraction and polarization. The second column of Table 1.1 contains the binding energy resolution after contraction. The third column shows the resolution after polarization is also added.

The spherical contraction of the hydrogen AO (second column) lowers the *interatomic* energy in two ways. Most importantly, *it increases the electron delocalization* between the quasi-atomic orbitals so that the negative kinetic interference energy is lowered by an additional −73.5 mh. The contraction also diminishes the quasi-classical electrostatic repulsion by −16.3 mh because of the increased shielding of the proton. This potential energy lowering is however smaller than the increase in the potential interference energy (+22.5 mh), which the aforementioned enhanced delocalization entails, so that the antibonding of the *total inter*atomic *potential* energy contribution increases by 6.1 mh. The total interatomic energy lowering by contraction is thus −67.4 mh and it is entirely due to the *kinetic* interference energy. This *interatomic* energy lowering is still stronger than the antibonding *intra-atomic* energy increase of 34.8 mh that occurs because AO contraction raises the intra-atomic kinetic energy more (by +298.8 mh) than lowering the intra-atomic potential energy (−264 mh), in agreement with the general discussion in Section 1.2.2. The net energy lowering due to contraction is thus −32.6 mh.

The polarization of the quasi-atomic orbitals (third column), on the other hand, lowers the *interatomic* quasi-classical electrostatic energy by −47.5 mh through shifting the *intra-atomic* charge on each nucleus slightly toward the other nucleus. However, polarization raises the negative interference energy by +23.9 mh so that the total *interatomic* energy is only lowered by −23.6 mh. Moreover, polarization increases the *intra-atomic* energy by +7.2 mh because it represents an intra-atomic charge shift that involves moving some electron population from a spherical orbital to higher angular momentum orbitals without orbital swelling. The net energy lowering due to polarization is thus only −16.4 mh.

1.4.7.4 **Variational Perspective**

The preceding analysis shows that, for every choice of quasi-atomic orbitals, *the interatomic kinetic energy change because of interference is the driving interaction, whereas the sum total of the interatomic potential interactions is always antibonding, as are of course the total intra-atomic energy changes*. Nonetheless, the *largest individual* energy changes are the *intra-atomic* changes in the kinetic and potential energies (+298.8 and −264 mh, respectively) and, although they nearly cancel each other, they actually invert the signs of the total contributions of **T** and **V** to the binding energy. This, somewhat puzzling, incidental result of the interplay between interatomic and intra-atomic energy changes can be understood by the following variational analysis.

In the molecule, the *interatomic* kinetic energy *lowering* is included in the variational competition between the total **T** and the total **V** and hence, the *intra-atomic* kinetic energy can *increase* beyond that of the free atom before the optimal compromise between **T** and **V** is reached. Hence, a contraction occurs that lowers the intra-atomic potential energy in a way similar to what would happen in a free atom when the kinetic energy resistance to localization is weakened by increasing the electron mass from 1 to about 1.275 (see Section 1.2.2). Thus, the *interatomic* kinetic energy lowering through delocalization can be said to open the possibility for an adjustment of the ratio between the *intra-atomic* electrostatic pull and kinetic resistance in the direction of a tighter attachment of the electron cloud to the nuclei than exists in the free atom, which leads to a corresponding energy lowering. One can also say that the weakening of the *overall* kinetic energy pressure resulting from *interatomic delocalization* allows for an increased *intra-atomic localization* through which the electron wave can exploit more effectively the attractive potential regions near the nuclei.

1.4.7.5 General Implications

One may reasonably ask whether the described interplay between interatomic and intra-atomic energy changes is a peculiar quirk of $H_2{}^+$ or whether it also occurs in other molecules. In this context, the virial theorem discussed in Section 1.2.3 is relevant. According to Eq. (1.9), the ratio $|2\mathbf{T}/\mathbf{V}|$ must be equal to 1 *at the equilibrium geometry of any molecule*. The following reasoning shows that this requirement entails the coupling of electron sharing and intra-atomic deformations, in particular, contraction.

From the first column of Table 1.1 it is seen that the *kinetic energy lowering* that results from electron sharing without quasi-atomic deformation, in conjunction with the concomitant *potential energy increase*, lowers the virial ratio $|2\mathbf{T}/\mathbf{V}|$ from the free-atom value 1 to the value 0.82 at the equilibrium distance. But it has to be 1 for the correct molecular wave function. According to the discussion in the second but last paragraph of Section 1.2.3, the exact wave function must therefore be more localized in regions of low potential energy. This localization is achieved by the intra-atomic contraction of the quasi-atomic orbitals, which entails the necessary large changes in the intra-atomic kinetic and potential energy (even though the total intra-atomic energy increase is small) that are needed to establish the virial ratio of 1.

In this regard, it is helpful to note that the contracted quasi-atomic orbital 1s* (second column of Table 1.1), which approximates the spherical component of the exact quasi-atomic orbital, is in fact very close to that contracted orbital $1s^\#$ that *minimizes the energy* of the approximate wave function $(1s_A{}^\# + 1s_B{}^\#)/\sqrt{(2 + 2S^\#)}$. [23] This orbital $1s^\#$ has the exponent $\zeta^\# = 1.240$, as compared to the exponent $\zeta^* = 1.264$ of 1s*, which was given at the end of Section 1.4.1. The corresponding molecular values of $\mathbf{E}^\#$, $\mathbf{T}^\#$, $\mathbf{V}^\#$ are therefore close to those for 1s*. Since energy optimization with respect to ζ guarantees the virial ratio $|2\mathbf{T}/\mathbf{V}| = 1$, this relation is indeed fulfilled by $\mathbf{T}^\#$ and $\mathbf{V}^\#$. It is therefore also justified to reason in terms of the variational competition between **T** and **V** with reference to the 1s* wave function listed in column 2 of Table 1.1. On the other hand, it is apparent that the proper compromise between electrostatic pull and kinetic resistance cannot be accomplished by a polarization deformation.

Finally, it is to be noted that the following relationships are *generally and rigorously valid*: (i) The virial ratio |**2T**/**V**| is equal 1 at all equilibrium geometries. (ii) Orbital exponent optimization always establishes the virial ratio. (iii) Electron delocalization always lowers the kinetic energy. In conjunction, these observations lead to the inference that any covalent bond that is formed by electron sharing, that is, delocalization, can be expected to involve orbital deformations that will attach the electrons more firmly to the nuclei. This anticipation will be confirmed by the analyses of the other molecules examined in Sections 1.5 and 1.6.

1.5
The Effect of Electronic Interaction in the Covalent Electron Pair Bond: H_2

Since the two electrons in the ground state of H_2 have opposite spins and, thus, are allowed to occupy the same function space, they are shared in a similar manner between the two atoms. The cumulative result of the bonding generated by each electron produces the pair bond. The binding energy analysis of H_2 is therefore very similar to that of H_2^+, showing that covalent bonding is also a one-electron phenomenon within an electron pair bond. However, electron sharing enhances the mutual interpenetration of the electrons, each of which originally resides on one atom, *and this enhanced penetration increases the interelectronic repulsion*. For this reason, the binding energy of H_2 is only 85% of twice the binding energy of H_2^+. The elucidation of this interelectronic effect is the new element to be traced in the analysis of H_2.

Following the approach laid out in Section 1.3.2, the binding energy of the optimal wave function in the FORS space will be analyzed first. This two-determinant wave function recovers 87.3% of the binding energy. The remaining 12.7%, contributed by the dynamic interelectronic correlation, will then be examined by means of a full CI wave function of 3176 determinants.

All the wave functions to be discussed were calculated using an uncontracted (14s, 6p, 3d, 2f, 1g) basis of 26 σ-type spherical Gaussian AOs on each atom, which was optimized for the present problem and differs slightly from that used for H_2^+.[1] It yields the energy −0.4999993 hartree and the virial ratio |**2T**/**V**| = 1.0000197 for the hydrogen atom. The quality of the present approach for the molecule was assessed by means of a full CI calculation at the internuclear distance $R = 1.4000$ Bohr, for which Kolos [24] as well as Nakatsuji [25], using the interelectronic distance in the wave function, have produced benchmark calculations of highest accuracy. The full

---

[1] The uncontracted basis set for H_2 was optimized to minimize the FCI energy at $R = 1.4$ bohr and contains GTOs with the following orbital exponents: $s = 26110.0$, 4078.0, 952.7, 243.8, 70.77, 23.75, 8.713, 3.628, 1.904, 1.243, 0.6419, 0.2978, 0.1382, 0.06620; $p = 11.13$, 3.858, 2.261, 1.079, 0.4752, 0.1952; $d = 3.111$, 1.232, 0.4749, $f = 2.661$, 0.9583, $g = 2.271$.

CI energy obtained with the present basis was found to lie 0.1991 mh above the value of −1.1744757 hartree determined by the two mentioned authors.

The FORS calculation yields the equilibrium distance 1.425859 Bohr, the energy of 1.1522764 hartree and the virial ratio $|2\mathbf{T}/\mathbf{V}| = 1.0000023$. The full CI calculation yields the equilibrium distance 1.4012 Bohr, the energy −1.1742769 hartree and the virial ratio $|2\mathbf{T}/\mathbf{V}| = 1.0000015$. The best bond length known is 1.4011 Bohr [26]. The quantitative details on which the discussion in the present section is based will be elaborated in a separate report [27].

1.5.1

Quasi-Atomic Orbitals of the FORS Wave Function

There are two atomic minimal basis set orbitals in this system. According to the discussion of Section 1.3.2, the FORS MO space is therefore by definition two-dimensional. It can be spanned by the bonding orbital σ_g and the antibonding sigma orbital σ_u, both of which are partially occupied. At all internuclear distances, this FORS wave function was obtained by MCSCF optimization of the expression

$$\Psi(1,2) = c_g\sigma_g(1)\sigma_g(2) + c_u\sigma_u(1)\sigma_u(2) \tag{1.43}$$

which determined the coefficients c_g, c_u as well as the orbitals σ_g, σ_u in terms of the 52-dimensional AO basis mentioned above. At the equilibrium distance, the coefficients are $\{c_g,\ c_u\} = \{0.99370277,\ -0.11204818\}$. The two quasi-atomic orbitals ψ_A, ψ_B that span the same FORS orbital space, that is, the QUAFOs, were then obtained as follows.

To determine ψ_A, the (2×26) overlap matrix between the MCSCF orbital set $(\sigma_g,\ \sigma_u)$ and the set of the 26 sigma basis AOs on atom A mentioned earlier was calculated. Its SVD yielded two orbitals in the FORS orbital space. At all internuclear distances, the largest SVD diagonal element is larger than 0.999780 (the value for 2.2 Bohr). The corresponding orbital in the FORS space is the QUAFO (quasi-atomic FORS orbital) ψ_A. The corresponding orbital that is spanned by the 26 basis AO's on atom A is the PAAO (Pure Atomic Approximate Orbital) to the QUAFO ψ_A. In contrast to the PAAO, the QUAFO contains a slight admixture from the basis AOs on atom B. In generalization of Eq. (1.11) for H_2^+, the QUAFO of H_2 on atom A can therefore be expressed as

$$\psi_A = a\mathbf{s}_A + b\mathbf{p}_A + \chi_B \tag{1.44}$$

$$\mathbf{s}_A = \sum(14\mathrm{s}_A), \quad \mathbf{p}_A = \sum(6\mathrm{p}_A, 3\mathrm{d}_A, 2\mathrm{f}_A, 1\mathrm{g}_A), \quad \chi_B = \sum(\text{orbitals on atom B}) \tag{1.44a}$$

where $\mathbf{s}_A$ and $\mathbf{p}_A$ are normalized. By expressing the spherical component $\mathbf{s}_A$ as the sum of a projection on the orbital $\mathbf{h}_A = 1s(H)$ of the free hydrogen atom A and its orthogonal complement, the Eq. (1.44) can be written

$$\psi_A = a\langle\mathbf{s}_A|\mathbf{h}\rangle\mathbf{h} + a(\mathbf{s}_A - \langle\mathbf{s}_A|\mathbf{h}\rangle\mathbf{h} + b\mathbf{p}_A + \chi_B \tag{1.44b}$$

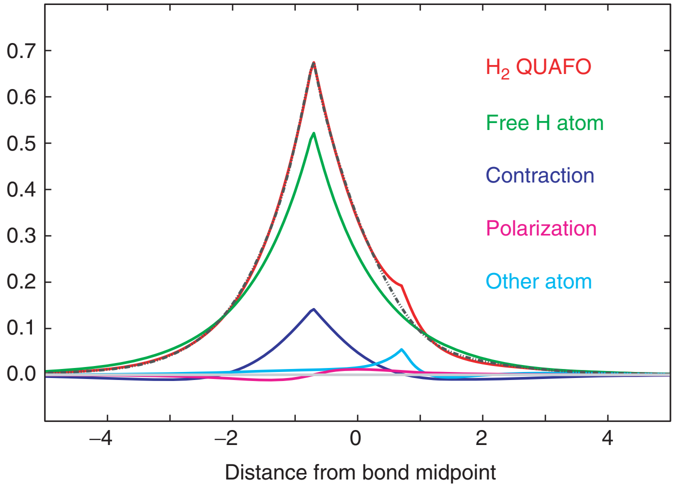

Figure 1.10 Resolution of the quasi-atomic FORS orbital (QUAFO) on the left atom in H_2 as a sum of contributions from the atomic 1s orbital, the spherical deformation, the angular deformation and the contribution from the right atom at the equilibrium distance. The dashed curve is the pure atomic approximate orbital (PAAO) to the QUAFO (see Section 1.5.1). Distances are in bohr from the bond midpoint.

The four terms of this resolution of ψ_A are displayed in Figure 1.10 for the equilibrium distance. It is apparent that, as in H_2^+, the second term represents a contraction of the spherical part.

Also shown in Figure 1.10, as a dotted curve, is the PAAO corresponding to the QUAFO ψ_A. The plot shows that the PAAO approximates the QUAFO extremely closely. The overlap integral between the two orbitals is 0.999865. A CI calculation of H_2 with the PAAOs yields an energy that is only 2 mh above that obtained with the QUAFOs, that is, the actual energy for Ψ.

The fractional contributions of contraction, polarization ($\mathbf{p}_A$), and the contribution from the other atom ($\boldsymbol{\chi}_B$) to ψ_A are exhibited in Figure 1.11 as functions of the internuclear distance. The values plotted in this Figure were obtained as follows. Since $\boldsymbol{\chi}_B$ is non-orthogonal to $\mathbf{s}_A$ and $\mathbf{p}_A$, the contribution from $\boldsymbol{\chi}_B$ that is actually different from the orbitals on A is given by $[\boldsymbol{\chi}_B - \langle\boldsymbol{\chi}_B|\mathbf{s}_A\rangle\mathbf{s}_A - \langle\boldsymbol{\chi}_B|\mathbf{p}_A\rangle\mathbf{p}_A]$ and this is the contribution shown in Figure 1.11. Accordingly, the contraction contribution shown is $[(a + \langle\boldsymbol{\chi}_B|\mathbf{s}_A\rangle)(\mathbf{s}_A - \langle\mathbf{s}_A|\mathbf{h}\rangle\mathbf{h})]$ and the polarization contribution shown is $[(b + \langle\boldsymbol{\chi}_B|\mathbf{p}_A\rangle)\ \mathbf{p}_A]$. It is apparent that, in H_2, the spherical contraction is of considerably greater relative importance than in H_2^+. The reasons will become apparent further on.

As in H_2^+, the spherical component $\mathbf{s}_A$ is very similar to a contracted hydrogen-like 1s orbital. Figure 1.12a shows the exponent ζ^* of this 1s* orbital, determined by maximizing the overlap of 1s* with $\mathbf{s}_A$ of Eq. (1.44a), as a function of the internuclear distance. The overlap between this 1s* orbital and the QUAFO ψ_A is

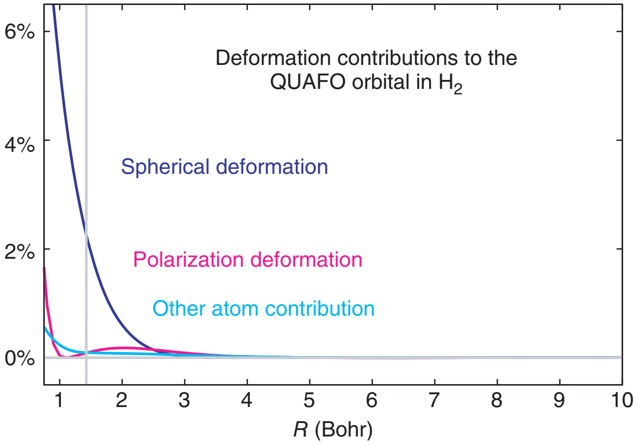

Figure 1.11 Variation with the internuclear distance for the spherical deformation, the angular deformations and the contribution from the other atom to the quasi-atomic orbital (QUAFO) in H_2. The gray vertical line indicates the equilibrium distance.

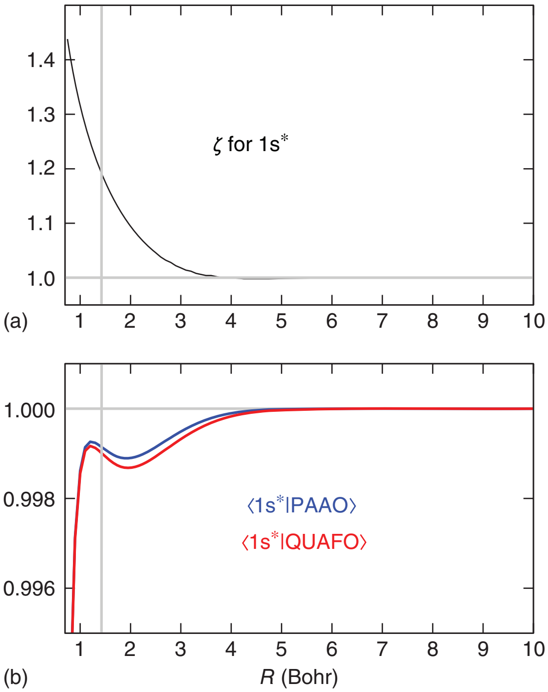

Figure 1.12 Characteristics of the scaled exponential approximation 1s* to the spherical part of the quasi-atomic orbital (QUAFO) in H_2 at various internuclear distances. (a) Orbital exponent of 1s*. (b) Overlap integral between the 1s* orbital and the quasi-atomic orbital (QUAFO) in red. Also shown: overlap integral between the 1s* orbital and the pure atomic orbital approximation (PAAO) to the QUAFO in blue.

shown in Figure 1.12b as a function of the distance. At the equilibrium distance the exponent of 1s* is $\zeta^* = 1.192$.

The QUAFO on atom B, ψ_B, was obtained in an entirely analogous way, using the 26 basis AOs on B for the SVD. The QUAFOs ψ_A and ψ_B were then chosen as the quasi-atomic basis to span the FORS space. They are related to the MCSCF bonding /antibonding MOs of Eq. (1.43) by the transformation

$$\psi_A = \sigma_g \cos\alpha + \sigma_u \sin\alpha \tag{1.45a}$$

$$\psi_B = \sigma_g \cos\alpha - \sigma_u \sin\alpha \tag{1.45b}$$

At the equilibrium distance, the value of $\cos\alpha$ is 0.920259 and the overlap integral between the non-orthogonal quasi-atomic orbitals is

$$S = \langle \psi_A | \psi_B \rangle = \cos 2\alpha = 0.693754 \tag{1.46}$$

With increasing internuclear distance, $\cos\alpha$ decreases to $1/\sqrt{2}$ and S decreases to zero.

1.5.2
FORS Wave Function and Density in Terms of Quasi-Atomic Orbitals

Using Eq. (1.45), the MCSCF optimized FORS wave function of Eq. (1.43) was then expressed in terms of the quasi-atomic orbitals, which yielded the valence-bond type expression

$$\Psi(1,2) = \left(\frac{N}{2}\right)^{\frac{1}{2}} \{\cos\gamma[\psi_A(1)\psi_B(2) + \psi_B(1)\psi_A(2)] + \sin\gamma[\psi_A(1)\psi_A(2) + \psi_B(1)\psi_B(2)]\} \tag{1.47}$$

$$N = \frac{1}{(1 + S^2 + 2S\sin 2\gamma)} \tag{1.48}$$

The coefficients $\cos\gamma$ and $\sin\gamma$ are related to the coefficients c_g, c_u, $\cos\alpha$, $\sin\alpha$ of Eqs. (1.43) and (1.45) by

$$\sin\gamma = \frac{C_1}{\sqrt{(C_1^2 + C_2^2)}} \qquad \cos\gamma = \frac{C_2}{\sqrt{(C_1^2 + C_2^2)}} \tag{1.49a}$$

$$4C_1 = \left(\frac{c_g}{\cos^2\alpha}\right) + \left(\frac{c_u}{\sin^2\alpha}\right), \quad 4C_2 = \left(\frac{c_g}{\cos^2\alpha}\right) - \left(\frac{c_u}{\sin^2\alpha}\right) \tag{1.49b}$$

At the equilibrium distance, the value of γ is 13.051068°.

The first order density matrix obtained from this wave function can be resolved into a quasi-atomic and an interference contribution between the quasi-atomic orbitals in a way that is entirely analogous to the corresponding resolution in H_2^+. One finds

$$\rho(1', 1'') = 2\int dx_2\, \Psi(1', 2)\Psi(1'', 2) = \rho_{qa}(1', 1'') + \rho_I(1', 1'') \tag{1.50}$$

where the quasi-atomic density matrix is the superposition of the atomic density matrices, that is,

$$\rho_{\mathrm{qa}}(1', 1'') = \psi_{\mathrm{A}}(1')\psi_{\mathrm{B}}(1'') + \psi_{\mathrm{B}}(1')\psi_{\mathrm{A}}(1'') \tag{1.51}$$

and the interference density matrix is

$$\rho_{\mathrm{I}}(1', 1'') = p \times \{[\psi_{\mathrm{A}}(1')\psi_{\mathrm{B}}(1'') + \psi_{\mathrm{B}}(1')\psi_{\mathrm{A}}(1'')] - S[(\psi_{\mathrm{A}}(1')\psi_{\mathrm{A}}(1'') + \psi_{\mathrm{B}}(1')\psi_{\mathrm{B}}(1'')]\} \tag{1.52}$$

with the *bond order*

$$p = \frac{(S + \sin 2\gamma)}{(1 + S^2 + 2S\sin 2\gamma)} \tag{1.53}$$

The diagonal terms, that is, the interference *density*, which is relevant for the potential energy terms, becomes therefore

$$\rho_{\mathrm{I}}(1, 1) = \rho_{\mathrm{I}}(1) = p \times \mathscr{I}_{\mathrm{AB}} \tag{1.54}$$

where

$$\mathscr{I}_{\mathrm{AB}} = 2\psi_{\mathrm{A}}\psi_{\mathrm{B}} - S(\psi_{\mathrm{A}}^2 + \psi_{\mathrm{B}}^2) \tag{1.54a}$$

is the same *orbital interference density* as the one that occurred in Eq. (1.14a) for H_2^+. The bond order p depends on the mixing ratio between the covalent and the ionic contribution to Ψ. For the Hartree–Fock wave function (i.e., $\gamma = 45°$ in Eq. (1.47)), it is $p = 1/(1 + S)$ so that the interference density expression of Eq. (1.54) becomes exactly twice that of H_2^+ given in Eq. (1.14). For the wave function of Eq. (1.47), it has the value 0.541996.

An implication of Eq. (1.54a) is that the orbital product $\psi_{\mathrm{A}}\psi_{\mathrm{B}}$ can be resolved into a coulombic and an interference component according to

$$2\psi_{\mathrm{A}}\psi_{\mathrm{B}} = S(\psi_{\mathrm{A}}^2 + \psi_{\mathrm{B}}^2) + \mathscr{I}_{\mathrm{AB}} \tag{1.54b}$$

This *interference resolution of the product* $\psi_{\mathrm{A}}\psi_{\mathrm{B}}$ will be used to analyze the role of the electron interaction terms in the binding energy analysis.

1.5.3
Binding Energy as a Sum of Two Intra-atomic and Five Interatomic Contributions

1.5.3.1 Overall Resolution

By inserting the discussed resolution of the density into the energy expression resulting from $\langle\Psi|\mathscr{H}|\Psi\rangle$ with the Hamiltonian of the H_2 molecule, and after appropriately combining terms, one obtains the following resolution of the binding energy in terms of contributions with physical meanings.

The total binding energy is again the sum of intra-atomic and interatomic energy changes and both are again resolved into kinetic and potential contributions:

$$\mathbf{E}_{\mathrm{Binding}} = \mathbf{E}(\Psi) - 2\mathbf{E}_{\mathrm{H}} = \mathbf{E}_{\mathrm{intra}} + \mathbf{E}_{\mathrm{inter}} \tag{1.55}$$

$$\mathbf{E}_{\mathrm{intra}} = \mathbf{T}_{\mathrm{intra}} + \mathbf{V}_{\mathrm{intra}} \tag{1.56}$$

$$\mathbf{E}_{\text{inter}} = \mathbf{T}_{\text{inter}} + \mathbf{V}_{\text{inter}} \tag{1.57}$$

The intra-atomic contributions are entirely analogous to those of H_2^+ in Eqs. (1.24), (1.31), and (1.37), except that, now, a full electron resides on each of the two atoms:

$$\mathbf{T}_{\text{intra}} = \frac{1}{2}\int dx(\nabla\psi_A)^2 + \frac{1}{2}\int dx(\nabla\psi_B)^2 - 1.0\,\text{Hartree} \tag{1.58}$$

$$\mathbf{V}_{\text{intra}} = -\int dx\frac{\psi_A^2}{r_A} - \int dx\frac{\psi_B^2}{r_B} + 2.0\,\text{Hartree} \tag{1.59}$$

The *interatomic kinetic energy* change is again the result of the interference of the quasi-atomic orbitals, that is,

$$\begin{aligned}\mathbf{T}_{\text{inter}} = \mathbf{T}_{\text{I}} = p \times \int dx \Big\{ 2\left(\psi_A\left(-\tfrac{1}{2}\nabla^2\right)\psi_B\right) \\ - \left[\left(\psi_A\left(-\tfrac{1}{2}\nabla^2\right)\psi_A\right) + \left(\psi_B\left(-\tfrac{1}{2}\nabla^2\right)\psi_B\right)\right]\Big\} \\ = p \times \frac{1}{2}\int dx\left\{2\left(\nabla\psi_A\right)\cdot(\nabla\psi_B) - [(\nabla\psi_A)^2 + (\nabla\psi_B)^2]\right\}\end{aligned} \tag{1.60}$$

where p is the bond order given in Eq. (1.53). Equation (1.60) is entirely analogous to Eq. (1.32) for H_2^+.

The *interatomic potential interactions* contain two kinds of terms, as was the case for H_2^+, namely:

- *coulombic* terms, which are defined as electrostatic interactions between *non-zero* charges,
- *interference* terms, that is, electrostatic interactions, which involve interference charge distributions that have *zero integrated charges* and describe *charge shifts with respect to the coulombic terms.*

Thus:

$$\mathbf{V}_{\text{inter}} = \mathbf{V}_{\text{coulombic}} + \mathbf{V}_{\text{interference}} \tag{1.61}$$

The contributions of the *interelectronic repulsion terms* to $\mathbf{V}_{\text{coulombic}}$ and $\mathbf{V}_{\text{interference}}$ are obtained by *substituting the interference Eq.* (1.54b) *for the orbital products* $\psi_A\psi_B$ *in the energy expression of* H_2.

1.5.3.2 Interatomic Coulombic Contributions

By the just mentioned substitutions, the total *coulombic* part of the interelectronic interaction is found to be

$$(1-2q)\langle\langle\psi_A^2|\psi_B^2\rangle\rangle + q\langle\langle\psi_A^2|\psi_A^2\rangle\rangle + q\langle\langle\psi_B^2|\psi_B^2\rangle\rangle \tag{1.62}$$

In this as well as the following equations of this section, light gray shading identifies terms arising from interelectronic interactions and the electrostatic integral between two charge distributions $f(x, y, z)$ and $g(x, y, z)$ is denoted by

$$\langle\langle f|g\rangle\rangle = \int dx_1 \int dx_2 \frac{f(1)g(2)}{|r_1 - r_2|} \tag{1.63}$$

The factors q and $(1-2q)$ in Eq. (1.62) have the following origin. Since *each* electron is *shared* between both atoms, *both* electrons contribute to the *average charge of 1e on each atom* and there exists a finite probability of finding both electrons on the same atom, that is, occupying the same quasi-atomic orbital. The analysis of the second-order density shows that (with N and γ being defined in Eqs. (1.47), (1.48) and (1.49))

$$q = \frac{(1-N\cos 2\gamma)}{4} \tag{1.64}$$

is the probability of finding both electrons on the same atom and, correspondingly, that $(1-2q)$ is the probability of finding one electron on atom A and the other on atom B. The value of q is maximal {viz 0.25} for the MO wave function ($\gamma = 45°$) and minimal, but not zero {viz $(S^2/4(1+S^2) = 0.081299$} for the valence bond (VB) wave function ($\gamma = 0°$). It is 0.142673 for the wave function of Eq. (1.47).

Combining the coulombic electron interaction terms of Eq. (1.62) with the electron nuclear *coulombic* attractions and the internuclear repulsion, the total *coulombic interaction* is expressed as follows

$$\mathbf{V}_{\text{coulombic}} = \mathbf{V}_{\text{qc}} + \mathbf{V}_{\text{sc}} \tag{1.65}$$

Where

$$\mathbf{V}_{\text{qc}} = -\int dx \frac{\psi_{\text{A}}^2}{r_{\text{B}}} - \int dx \frac{\psi_{\text{B}}^2}{r_{\text{A}}} + \langle\langle \psi_{\text{A}}^2 | \psi_{\text{B}}^2 \rangle\rangle + \frac{1}{\text{R}}$$

= the quasi-classical coulombic interaction between the two atoms, each having one full electron (1.66)

$$\mathbf{V}_{\text{sc}} = q \times \left\{ \langle\langle \psi_{\text{A}}^2 | \psi_{\text{A}}^2 \rangle\rangle + \langle\langle \psi_{\text{B}}^2 | \psi_{\text{B}}^2 \rangle\rangle - 2\langle\langle \psi_{\text{A}}^2 | \psi_{\text{B}}^2 \rangle\rangle \right\}$$

= a “correction” of the preceding term $\mathbf{V}_{\text{qc}}$ so that the sum of the interelectronic terms in $\mathbf{V}_{\text{coulombic}}$ of Eq. (1.65) becomes in fact identical with the actual terms given in Eq. (1.62) (1.67)

The quasi-classical coulombic term $\mathbf{V}_{\text{qc}}$ of Eq. (1.66) has been formulated so as to balance attractions and repulsions between the atoms in a way analogous to the quasi-classical interaction term in H_2^+ given in Eq. (1.25). The term $\mathbf{V}_{\text{sc}}$ manifestly *replaces* an appropriate amount of *interatomic* electron repulsion, included by definition in $\mathbf{V}_{\text{qc}}$, with the amount of *intra-atomic* electron repulsion required to recover the *actual* contribution given in Eq. (1.62). Since the *intra-atomic* electron repulsions are generated by electron sharing, the energy contribution $\mathbf{V}_{\text{sc}}$ is called the *coulombic sharing contribution*. It is the energetic measure of the finite probability of both electrons being on the same atom. Although rarely mentioned, it is quite strong and antibonding.

1.5.3.3 **Interatomic Interference Contributions**

The *potential interference energy* is the sum of two contributions

$$\mathbf{V}_{\text{interference}} = \mathbf{V}_{\text{I}} + \mathbf{V}_{\text{II}} \tag{1.68}$$

The first term is analogous to the potential interference energy of $H_2{}^+$ given by Eq. (1.26). Here, one obtains

$$\begin{aligned}\mathbf{V}_\mathrm{I} &= \int \mathrm{d}x \left(-\frac{1}{r_\mathrm{A}} - \frac{1}{r_\mathrm{B}}\right) \rho_\mathrm{I} + \frac{1}{2}\langle\langle \psi_\mathrm{A}^2 + \psi_\mathrm{B}^2 | \rho_\mathrm{I}\rangle\rangle \\ &= p \times \left\{ \int \mathrm{d}x \left[\left(-\frac{1}{r_\mathrm{A}} - \frac{1}{r_\mathrm{B}}\right) \mathscr{I}_\mathrm{AB} + \frac{1}{2}\langle\langle \psi_\mathrm{A}^2 + \psi_\mathrm{B}^2 | \mathscr{I}_\mathrm{AB}\rangle\rangle \right]\right\} \end{aligned} \tag{1.69}$$

where ρ_I and $\mathscr{I}_\mathrm{AB}$ are the orbital interference terms of Eqs. (1.54) and (1.54a) and p is the bond order of Eq. (1.53). The difference between this expression for $\mathbf{V}_\mathrm{I}$ and that for $H_2{}^+$ in Eq. (1.26) is the presence of the electron repulsion terms $\langle\langle..|..\rangle\rangle$, which have the following origin: The interference density of each electron experiences the attractions of the two *shielded* nuclei. The shielding that one electron experiences is caused by the coulombic repulsion of the other electron, which is evenly distributed over both nuclei, so that each nucleus is shielded by half an electron.

The second interference term in Eq. (1.68) is

$$\mathbf{V}_\mathrm{II} = \frac{1}{4} N \langle\langle \mathscr{I}_\mathrm{AB} | \mathscr{I}_\mathrm{AB}\rangle\rangle \tag{1.70}$$

It represents the interaction between the interference energies of the two electrons.

1.5.3.4 Binding Energy as a Sum of Two Intra-atomic and Five Interatomic Contributions

The total binding energy is then the sum of the following seven contributions with physical interpretations discussed in Sections 1.5.3.1 to 1.5.3.3:

$$\mathbf{E}_\mathrm{Binding} = \mathbf{T}_\mathrm{intra} + \mathbf{V}_\mathrm{intra} + \mathbf{T}_\mathrm{I} + \mathbf{V}_\mathrm{qc} + \mathbf{V}_\mathrm{sc} + \mathbf{V}_\mathrm{I} + \mathbf{V}_\mathrm{II} \tag{1.71}$$

This decomposition has not been arbitrarily conceived or imposed. Rather, it is the result of simply sorting out the terms in the rigorous energy expression $\langle\Psi|\mathscr{H}|\Psi\rangle$ after inserting the interference resolution of Eq. (1.54b) for $\psi_\mathrm{A}\psi_\mathrm{B}$.

1.5.4

Quantitative Synergism of the Contributions to the Binding Energy

1.5.4.1 Quantitative Characteristics

From the discussion in the preceding section it is apparent that five of the seven contributions to the binding energy Eq. (1.70), namely $\mathbf{T}_\mathrm{intra}$, $\mathbf{V}_\mathrm{intra}$, $\mathbf{V}_\mathrm{qc}$, $\mathbf{T}_\mathrm{I}$, $\mathbf{V}_\mathrm{I}$, have the same physical meanings as the corresponding contributions in $H_2{}^+$, which were discussed in Section 1.4.4.

These contributions also exhibit the same general *quantitative* characteristics as those discussed for $H_2{}^+$ in Section 1.4.5. An exception is the quasi-classical coulombic energy $\mathbf{V}_\mathrm{qc}$, which differs from twice that of $H_2{}^+$ in that one *internuclear* repulsion is replaced by the *interelectronic* repulsion, as is seen by comparing the definition of Eq. (1.66) for H_2 with that of Eq. (1.25) for $H_2{}^+$. As a consequence and in contrast to $H_2{}^+$, the term $\mathbf{V}_\mathrm{qc}$ is, therefore, *always* attractive in H_2.

More importantly, the binding energy of Eq. (1.71) also contains the *coulombic sharing contribution* $\mathbf{V}_{\mathrm{sc}}$ of Eq. (1.67), which does not exist in H_2^+. It arises from both electrons spending part of the time simultaneously on the same atom. As explained after Eq. (1.67), it replaces an *interatomic* electron repulsion by *intra-atomic* repulsions. Since the latter are significantly larger than the former, this term is always positive, that is, antibonding. As a result the *sum total coulombic contribution* $\boldsymbol{V}_{coulombic} = \boldsymbol{V}_{qc} + \boldsymbol{V}_{sc}$ *of Eq. (1.65) is in fact antibonding at all internuclear distances*, even when the quasi-atomic orbitals are polarized. It is a two-electron price to be paid for the energy lowering gained by simultaneous one-electron sharing of the two electrons in the same bond. The compromise between $\mathbf{V}_{\mathrm{sc}}$ and the interference energy $\mathbf{T}_{\mathrm{I}}$ determines what is sometimes called *left–right correlation*.

Finally, the binding energy of Eq. (1.70) contains the second interference term $\mathbf{V}_{\mathrm{II}}$. It represents the self-energy of a distribution with zero total charge and is therefore expected to have very small numerical values.

1.5.4.2 **Synergism along the Dissociation Curve**

The synergism of the various contributions to the binding energy is shown in Figure 1.13 for H_2, which corresponds to Figure 1.9 for H_2^+. The rows and columns of the 15 panels have exactly the same meaning as in Figure 1.9 and were explained in detail in the second paragraph of Section 1.4.6. The comparison of the two figures shows that, notwithstanding differences in quantitative details, all binding energy contributions exhibit essentially the same bonding and antibonding pattern over the full range of the interatomic distance.

The differences between H_2 and H_2^+, which are a result of the presence of the interelectronic repulsions, appear mainly in the panels of the first row, that is, for the coulombic contributions. Whereas only the quasi-classical coulombic term $\mathbf{V}_{\mathrm{qc}}$ is present in H_2^+, the coulombic contribution of H_2 contains in addition the coulombic sharing contribution $\mathbf{V}_{\mathrm{sc}}$. In confirmation of the explanation elaborated in the preceding Section 1.5.4.1, it is seen that, *at all distances and on all three panels, i.e., for all three quasi-atomic orbital choices, the quasi-classical term* $\boldsymbol{V}_{qc}$ *is attractive, the sharing modification* $\boldsymbol{V}_{sc}$ *is repulsive and the total coulombic contribution* $\boldsymbol{V}_{coulombic}$ *is repulsive*. Nonetheless, when the spherical 1s* quasi-atomic orbital approximation (second column) is replaced by the polarized exact quasi-atomic orbitals (third column), the coulombic contributions of H_2 and H_2^+ change in the same direction: In H_2^+, the contribution changes from repulsive to attractive; in H_2, it becomes less repulsive. Specifically, the quasi-classical term of H_2 becomes more attractive and the coulombic sharing contribution becomes less antibonding. Thus, in both molecules, the polarization of the quasi-atomic orbitals, which results from replacing the 1s* quasi-atomic orbital approximation (second column) by the exact quasi-atomic orbitals (third column), lowers the binding energy because it lowers the coulombic energy. This lowering outweighs the increases in the interference energy and the intra-atomic energy caused by the polarization as discussed in

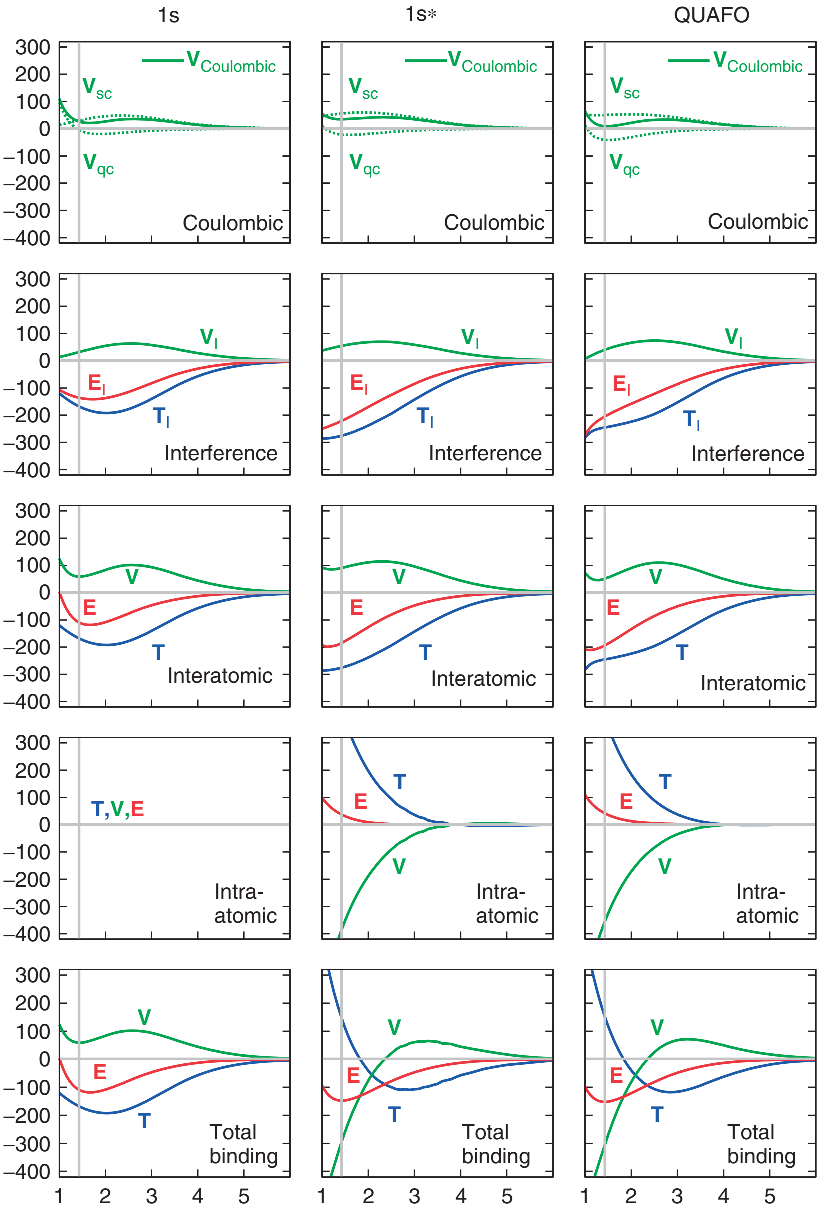

Figure 1.13 Each *column of panels* exhibits the contributions to the binding energy of H_2 as functions of the interatomic distance. First column: when the molecular wave function is a superposition of atomic ground state 1s orbitals. Second column: when the molecular wave function is a superposition of the scaled exponential 1s* approximations to the QUAFOs (see Figure 1.12). Third column: when the molecular wave function is a superposition of the QUAFOs, that is, for the actual wave function.

Section 1.4.6.3. Nonetheless, the total inter-atomic potential contribution to the binding energy remains anti-bonding over the whole range.

As noted earlier, the second interference term is expected to have very small values. In fact, these values are so small that they are indistinguishable from zero on the scale of the panels in the second row *in Figure* 1.13 and are therefore not displayed. The total potential interference energy shown in these panels is therefore essentially equal to $\mathbf{V}_\mathrm{I}$ of Eq. (1.69).

The overall synergism of the binding energy contributions in H_2 is thus the same as that in H_2^+ and the general conclusions deduced for H_2^+ by the in-depth discussions in Sections 1.4.5 and 1.4.6 apply therefore also to H_2.

1.5.5

Origin of Bonding at the Equilibrium Distance

Detailed insights into the effect of the interelectronic interaction on the binding energy are provided by the explicit quantitative values at the equilibrium distance, which are listed in Table 1.2. The table is analogous to Table 1.1 for H_2^+ and is organized in the same manner. The rows and columns have the same meaning in the two tables and they also correspond to those in Figure 1.13, which was discussed in the preceding Section 1.5.4.2.

Table 1.2 Binding energy analysis of H_2 at R_{eq} (energies in mh).

Atomic orbitals used → **Interaction type ↓**		**Free atoms**	**Contracted free atoms**	**Quasi-atoms in molecule**
Quasi-classical coulombic	**V**	–4.7	–21.6	–41.0
Sharing Coulombic	**V**	30.8	56.2	50.4
Interference I	**T**	–167.8	–275.7	–245.0
	V	31.6	54.7	40.2
	E	–136.2	–221.0	–204.8
Interference II	**V**	1.0	1.6	1.6
Interatomic total	**T**	–167.8	–275.7	–245.0
	V	58.7	90.9	51.2
	E	–109.1	–184.8	–193.8
Intra-atomic	**T**	0	420.9	397.3
	V	**0**	–384.0	–355.8
	E	0	36.9	41.5
Total binding	**T**	–167.8	145.2	152.282
	V	58.7	–293.1	–304.559
	E	–109.1	–147.9	–152.276

The overall quantitative energetic pattern is indeed analogous to that found for H_2^+. In particular the *interatomic* energy lowering is the driver for all three quasi-atomic orbital choices (columns). There are however noteworthy differences.

1.5.5.1 The Primary Mechanism as Exhibited by Choosing the Free-Atom Orbitals as Quasi-Atomic Orbitals

As in H_2^+, the binding energy in the first column of Table 1.2 is again furnished by the *kinetic interference* energy (−167.8 mh), that is, electron delocalization. It is 54.1 mh more bonding than that of H_2^+ (−113.7 mh). But the former is less than twice the latter, presumably because the bond order p of H_2 [~0.542 see after Eq. (1.54a)] is less than twice that in H_2^+ [~0.315, see after Eq. (1.14a)].

On the other hand, the antibonding *potential interference* energy in H_2 (+31.6 + 1.0 = +32.6 mh) differs only by 0.2 mh from that of H_2^+, even though two electrons are involved. The reason is presumably that the potential acting on the interference density ρ_I of H_2 in Eq. (1.69) is weaker than the corresponding potential for H_2^+ in Eq. (1.26) because, in H_2, each nucleus is shielded by half an electron as explained after Eq. (1.69).

Although the *quasi-classical* coulombic energy of H_2 is attractive (−4.7 mh), as explained in Section 1.5.4.1, and in fact 32.3 mh lower than the repulsive quasi-classical energy in H_2^+, the *total coulombic* energy of H_2 is repulsive (+26.1 mh) and only 1.5 mh lower than that of H_2^+. This is because of the additional coulombic repulsion that is a result of the finite probability of both electrons being on the same atom, as explained in the third paragraph of Section 1.5.4.1. It gives rise to the antibonding *coulombic sharing energy* $\mathbf{V}_{sc}$, of +30.8 mh!

As a result the interatomic *potential* contributions add up to the antibonding value of +58.7 mh against the bonding *kinetic* contribution of −167.8 mh, yielding the binding energy of −109.1 mh.

1.5.5.2 Effect of Quasi-Atomic Orbital Contraction

As discussed in detail in Section 1.4.3, near the equilibrium distance the contraction shown in the second column of Table 1.2 enhances interference, delocalization and charge accumulation in the bond. As in H_2^+, the *kinetic interference energy* is thus enhanced to −275.7 mh, that is, by a factor 1.64, which is near identical to the corresponding enhancement factor in H_2^+. The antibonding *potential interference energy* increases by a factor 1.73, which is also similar to that factor in H_2^+.

The contraction lowers the *quasi-classical coulombic* energy by −16.9 mh (second minus first column), that is, by almost the same amount as in H_2^+ (−16.3 mh). On the other hand however, it is manifest from the Eq. (1.67) and the subsequent discussion that quasi-atomic orbital contraction will *increase the sharing coulombic energy* $\mathbf{V}_{sc}$. This increase is in fact 25.4 mh so that the antibonding of the *total coulombic energy increases* by +8.5 mh. In H_2^+ by contrast, where $\mathbf{V}_{sc}$ does not exist, the coulombic energy *decreases* by −16.3 mh.

As a result, contraction increases the total antibonding *interatomic potential* contributions by a factor 1.54 in H_2 as compared to a factor of only 1.1 in H_2^+. Since contraction increases the bonding *interatomic kinetic* contributions in H_2

and H_2^+ by the same factor (about 1.7, see two paragraphs earlier), contraction enhances the *total interatomic* bonding contribution of H_2 (−184.8) only by a factor 1.69 whereas that factor is 2.26 in H_2^+.

Contraction increases the intra-atomic energy by +36.9 mh, which is only 2.1 mh more than that in H_2^+ (the contraction is less than in H_2^+, but two electrons contribute).

As a result, the total binding energy of H_2 (−147.9 mh) has been enhanced by a factor of 1.36 through quasi-atomic orbital contraction. This factor is less than the factor 1.61 in H_2^+.

1.5.5.3 **Effect of Polarization**

The third column of Table 1.2 shows the effect of modifying the quasi-atomic orbitals by polarization as well as by the admixture from the other atom. For simplicity, both distortions of the exact quasi-atomic orbitals' spherical symmetry will be subsumed under the label ''polarization'' in the following paragraphs.

The effect of these distortions on the interference energy of H_2 is very similar to that in H_2^+: The kinetic interference contribution becomes less bonding, the potential interference contribution becomes less antibonding and the total interference energy becomes less bonding, that is, more positive. The increase in the value of the interference energy in H_2 (16.2 mh) is less than the corresponding increase in H_2^+ (23.9 mh).

As in H_2^+, polarization lowers the quasi-classical coulombic energy of H_2, that is, it makes it more bonding. But the energy lowering is less than half of that in H_2^+. It also lowers the antibonding sharing coulombic energy somewhat. The total coulombic energy lowering through polarization in H_2 (−25.2 mh) is considerably less than that in H_2^+ (−47.5 mh).

As a result the *total interatomic* bonding interactions in H_2^+ are enhanced by only −9.0 mh as compared to −23.6 mh in H_2^+.

Polarization increases the *intra-atomic* antibonding 4.6 mh, that is, 2.6 mh less than in H_2^+.

As a result, the *total binding energy* of H_2 is enhanced only by −4.4 mh through polarization whereas the enhancement in H_2^+ is −16.4 mh. The effect of the distortion of the quasi-atomic orbitals from spherical symmetry is thus much smaller in H_2 than in H_2^+.

1.5.5.4 **Binding in the Electron Pair Bond of H_2**

As in H_2^+, the driving element of binding in H_2 is the interatomic *kinetic* energy lowering through delocalization (''electron sharing''), which is embodied in the kinetic interference energy. This effect is a part of the cumulative *one-electron* energies of the two electrons. The two-electron bond is thus the cumulative result of the one-electron bonding created by each electron. The essential conclusions regarding the origin of the covalent bond in H_2^+, which were summarized in Section 1.4.7, remain therefore also valid for H_2.

These one-electron bonding effects are however diminished by the presence of the interelectronic repulsion because the bonding delocalization of *both* electrons also results in a finite probability of the two electrons being found at the same atom, and this simultaneous presence at the same site generates a strong coulombic repulsion that exists neither in the hydrogen atoms nor in the H_2^+ molecule. In consequence, the binding energy of H_2 is less than twice that of H_2^+.

In the energy analysis, the effects caused by the interelectronic repulsion appear in three places:

1) The *strong* antibonding contribution generated by the finite probability of finding both electrons near the same nucleus is embodied in the sharing coulombic energy $\mathbf{V}_{sc}$, which is absent in H_2^+. Indeed, the value of $\mathbf{V}_{sc}$ at the equilibrium distance, viz 50.4 mh (Table 1.2) is very close to the difference of 52.0 mh between the binding energy of the FORS wave function (Table 1.2) and twice the binding energy of H_2^+ (Table 1.1).
2) Because of the electron repulsion, the delocalization of the individual electrons is moreover not as uninhibited as in H_2^+, a fact often denoted as "left–right correlation" As a result, the bond order, which weights the interference terms, is smaller than twice that in H_2^+.
3) The nuclear potentials that act on the interference density are shielded, which reduces the antibonding *potential* energy increase associated with the charge accumulation in the bond. But this enhancement of bonding is counteracted by the bond order attenuation mentioned under (ii) which decreases the bonding of the *kinetic* interference terms.

It should be noted that the large antibonding term $\mathbf{V}_{sc}$ is a *coulombic* interaction. Although it is generally appreciated that the *quasi-classical* coulombic energy is attractive in H_2, it seems to be much less recognized that electron sharing also generates the large repulsive coulombic term $\mathbf{V}_{sc}$ and that, in consequence, the *total coulombic contribution* is in fact always antibonding – in contrast to H_2^+, where it is bonding. In fact, as in H_2^+, the sum total of the inter-atomic potential contributions is always anti-bonding.

1.5.6
Electron Correlation Contribution to Bonding in H_2

As seen in the preceding parts of this section, the finite probability of both electrons being on the same atom, which is inherent in the FORS wave function, entails an electron repulsion that causes the FORS binding energy (−152.276 mh) to fall 52 mh short of twice the binding energy of H_2^+ (−102 mh). Of this difference, 22 mh are recovered by the exact wave function, in which the probability of the two electrons to find themselves in the same space element is reduced by adjustments beyond the FORS level, that are termed *dynamic correlations*. Thus, 87% of the actual binding energy (−174.476 mh) is accounted for at the FORS level and 13% is recovered by dynamic correlation.

To examine the correlating adjustments, a full configuration interaction (FCI) wave function was calculated in the configuration space spanned by the 3176 determinants that are generated by the 140 orbitals of the 14s, 6p, 3d, 2f, 1g basis mentioned in the third paragraph of Section 1.5. It yields the binding energy −174.168 at the FORS equilibrium distance (1.425859 Bohr), and −174.277 mh at the re-optimized equilibrium distance (1.4012 Bohr).

At the FORS equilibrium distance, where the FCI wave function recovers 99.8% of the binding energy, the dominant FCI natural orbitals (NOs) and their occupations are:

$1\sigma_g$	$1\sigma_u$	$2\sigma_g$	$1\pi x_u$	$1\pi y_u$	135 remaining NOs
1.96347	0.02067	0.00598	0.00428	0.00428	0.00132

The first two of these NOs closely resemble the bonding and antibonding FORS orbitals and account for 1.98414 electrons. The next three natural orbitals provide in–out and π angular correlation. The two configurations that form the FORS wave function clearly represent the dominant part of the nearly exact FCI function. According to the text after Eq. (1.43), the occupancies of the corresponding two NOs in the FORS wave function are 1.974890, and 0.025110.

To assess the effect of dynamic correlation on the bonding interactions at the equilibrium distance, the interference effects generated by the FCI wave function are compared with those of the FORS wave function in Figure 1.14. The interference densities, which show the charge accumulation in the bond, and the kinetic interference densities, which exhibit the effect of delocalization on the kinetic energy, were calculated as follows:

$$\text{Interference density} \qquad \sum_i^N n_i\phi_i^2 - \psi_A^2 - \psi_B^2$$

$$\text{Kinetic interference density} \qquad +\frac{1}{2}\sum_i^N n_i\{\nabla\phi_i\}^2 - \frac{1}{2}\{\nabla\psi_A\}^2 - \frac{1}{2}\{\nabla\psi_B\}^2$$

where the ϕ_i are the respective NOs, the n_i are their occupations and ψ_A and ψ_B are the QUAFO orbitals determined in Section 1.5.1. The upper limit N is 2 and 140 for the FORS and the FCI case respectively. These contour plots are analogous to those shown in Figure 1.6 for H_2^+.

It is apparent from the first two rows of panels in Figure 1.14 that the two-electron correlation effects modify the basic structure of the one-electron densities so little that the changes are hardly perceptible on the scale of these plots. The difference plots displayed in the third row have reduced contour increments: 4 times reduced on the left panel, 10 times reduced on the right panel. The result of electron correlation is seen to enhance very slightly the charge accumulation in the bond (lower left panel). As argued in Section 1.4.5.3 and shown by the subsequent quantitative results (e.g., Figures 1.9, 1.13 and Tables 1.1, 1.2), this enhancement is expected to slightly increase the (positive) potential energy. On the other hand, the correlation modification of the wave function slightly increases the gradient density in a very narrow region near the nuclei (lower right panel, in agreement

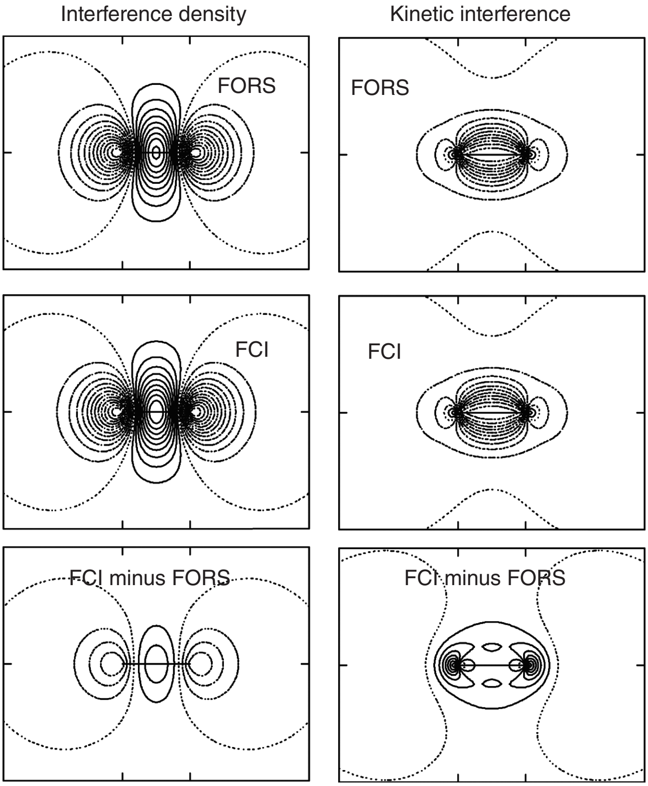

Figure 1.14 Comparison of the interference for the full CI wave function with that for the FORS wave function of H_2. Left column of panels: interference densities with contour increments = 0.004 e Bohr^{-3} in the upper two panels and 0.001 e Bohr^{-3} in the lowest panel. Right column of panels: kinetic interference densities with contour increments = 10 millihartree Bohr^{-3} in the upper two panels and 1 millihartree Bohr^{-3} in the lowest panel. Note that the increment in the upper four panel's is twice that used for the one-electron system H_2^+ in Figure 1.6.

with the lower left panel), which is expected to also increase the kinetic interference density slightly.

These inferences are confirmed by the decomposition of the binding energy in terms of its kinetic (**T**), nuclear-electronic attraction ($\mathbf{V}_{ne}$), and electron–electron repulsion contributions ($\mathbf{V}_{ee}$), which is documented along the internuclear distance in Figure 1.15. The two dissociation graphs at the top show that the relative roles of these three components are very similar in the FCI and the FORS wave function over the whole range.

The lower panel exhibits the modifications induced by the full CI calculations on a scale that is magnified by a factor 20. At the equilibrium distance, the one-electron energy changes are as predicted earlier from the interference plots in Figure 1.14. The increases of the one-electron energies **T** and $\mathbf{V}_{ne}$ are manifestly a side effect of the much larger lowering of the electron repulsion energy $\mathbf{V}_{ee}$ that is achieved

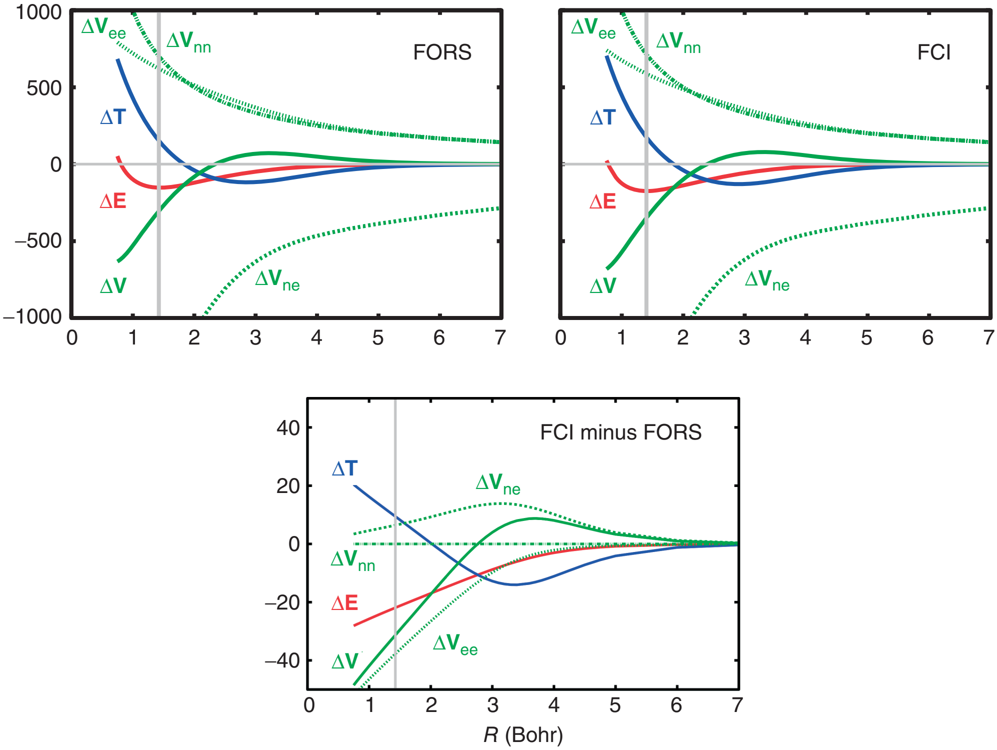

Figure 1.15 Comparison of the kinetic, potential, and total energies of the full CI wave function with those of the FORS wave function. Energy scale in millihartree.

by the correlating wave function adjustments. At large distances (>5 Bohr), on the other hand, the one-electron FCI energies still differ by about 5 micro-hartree from the corresponding FORS energies, even though the electronic interaction energy differs by less than one micro-hartree. This surprizing result may be related to the very long range of the (small) polarization effect that was noted in Figure 1.11.

The correlating wave function adjustments manifestly do not change the physical interactions that lead to bond formation at the FORS level. These interactions between the atomic minimal basis sets are left intact and remain dominant. The correlating adjustments achieve however a reduction of about 40% in the amount by which the bond energy of H_2 falls short of twice the bond energy of H_2^+.

1.6
Covalent Bonding in Molecules with More than Two Electrons: B_2, C_2, N_2, O_2, and F_2

The essential conclusion of the preceding analysis has been that covalent bond formation in H_2^+ and H_2 is the consequence of the attenuation of the kinetic energy pressure experienced by each electron due to its *interatomic* delocalization (“sharing”). This attenuation is further enhanced by intra-atomic contractions, which moreover allow the electronic wave to exploit more of the attractive potentials near the nuclei. The shrinkage toward the nuclei is signaled by large contragredient changes in the intra-atomic kinetic and potential energies. Although these changes are large, they are not the cause of the binding process inasmuch as they nearly cancel each other, leaving a small antibonding contribution. In the last paragraph of Section 1.4, it was argued that this process of covalent bonding is general. In the present section, it will be shown that, in the five diatomic molecules $B_{2,}$ $C_{2,}$ N_2, O_2, and F_2, covalent bonding involves, in fact, the same pattern of energy changes and thus comes about in the same way.

All molecules are treated at the full valence space MCSCF level, that is, the full FORS wave functions based on eight molecular valence orbitals is analyzed. In addition a wave function containing some additional valence correlation is considered for $F_{2.}$ All calculations are performed with Dunning’s quadruple-zeta cc-pVQZ basis sets [28] using the GAMESS molecular program suite [29].

1.6.1
Basis of Binding Energy Analysis

The detailed interactions in these systems are manifestly quite complex and a complete analysis is beyond the scope of this chapter. Only those aspects will be exhibited that have a bearing on the essential basic mechanism summarized in the first paragraph of this section. To this end, the following four energies are calculated for each molecule.

Energy (i): The energy of the *free atom* is calculated at the full valence space MCSCF level (FORS), the core being kept as a closed shell. This calculation is performed assuming the configurational structure that will result for the atom when the molecular calculation is done at large internuclear distances. Accordingly, the atomic calculation is performed in $C_{\infty v}$ symmetry, keeping the orbitals p_x and p_y equivalent, but the p_z orbital nonequivalent. The five minimal basis set orbitals are optimized in the quadruple-zeta AO basis (55 orbitals) of the atom.

Energy (ii): The energy of the *molecule* is calculated by a full valence space MCSCF calculation, the cores being closed shells. However, in this calculation the orbitals *are not optimized in the quadruple-zeta AO bases*. Rather, *all 10 orbitals* are determined as optimal linear combinations of the 10 optimal (core and valence) free-atom orbitals that were found in the preceding atomic calculations on the two atoms. The resulting molecular wave function represents the analogue to the wave function that was obtained for H_2 with the 1s ground state orbital of the hydrogen atom.

Energy (iii): The energy of the *molecule* is optimized by a full valence space MCSCF calculation, the cores being closed shells. In this calculation the orbitals are optimized in the full quadruple-zeta bases of both atoms. This is the FORS energy of the molecule.

Energy (iv): The energy of the *quasi-atom in the molecule* is determined, which represents the analogue to the quasi-atomic energies obtained in H_2^+ and H_2 by using the (contracted + polarized) quasi-atomic orbitals. This objective is accomplished as follows.

The first step is to determine a basis for quasi-atomic FORS orbitals (QUAFO's) that span the full FORS function space of the MCSCF MOs obtained in the preceding calculation (iii). To this end, the overlap integral matrix is calculated between, on the one hand, all 10 *molecular* FORS MCSCF orbitals (including the core orbitals) and, on the other hand, *all 55 orthogonal occupied and virtual free-atom orbitals obtained earlier in calculating the energy (i) on one of the two atoms*. Then, the SVD of this matrix is performed and those five MOs that correspond to the largest five SVD eigenvalues are taken as the optimal quasi-atomic orbital basis on that atom. By an analogous procedure, five quasi-atomic orbitals are determined for the other atom. The ten quasi-atomic orbitals obtained in this manner span the same orbital space as the molecular FORS orbitals from the molecular MCSCF calculation of step (iii). We consider these QUAFOs as the quasi-atomic orbital basis that is intrinsically embedded in the FORS wave function.

As typical examples, Figure 1.16 displays contours of the quasi-atomic MOs for the molecules N_2 and F_2. For N_2, all five QUAFOs on one atom are shown. The figure for F_2, on the other hand, omits the 1s and the equivalent p_y orbitals. It displays the three quasi-atomic FORS orbitals 2s, $2p_z$ and $2p_x$ and the two additional correlating orbitals 3s and $3p_x$, which were obtained from a wave function that included some valence correlation (see Section 1.6.4). The correlating quasi-atomic orbitals were obtained by an entirely analogous SVD algorithm involving 16 MCSCF orbitals. In view of the manifest atomic localization of these orbitals, we emphasize that all of them are *MO*s in terms of which the molecular wave functions can be expressed.

The energy of each quasi-atom in the molecule is then obtained by a full valence space MCSCF (FORS) atomic calculation with the same format as that used for the atomic calculation of Energy (i). However, the orbitals *are not optimized in the quadruple-zeta AO basis*. Rather, *all five orbitals* are determined as *optimal linear combinations of the five QUAFOs* that were obtained for that atom as described in the preceding paragraph.

1.6.2
Origin of Binding at the Equilibrium Geometry

The results obtained by these calculations for the five molecules at their theoretical equilibrium distances are contained in Table 1.3. For comparison, the corresponding values of H_2 are also included. Because the quantities of interest are the binding energies, all entries listed in this table are in fact energies *with reference to twice the free-atom energy*, i.e., 2 × Energy (i) of the preceding Section 1.6.1 has been subtracted from all energies.

Quasi-atomic orbitals on the left atom of N_2: FORS calculation

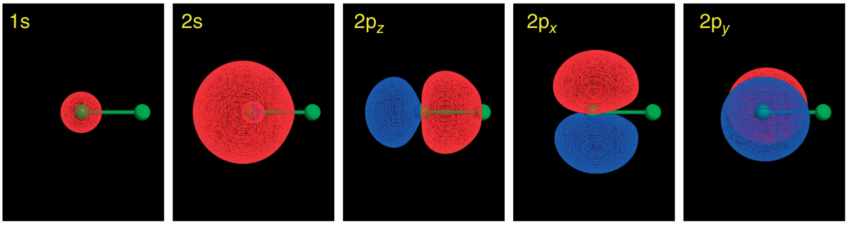

Quasi-atomic orbitals on the left atom of F_2: correlated FORS calculation

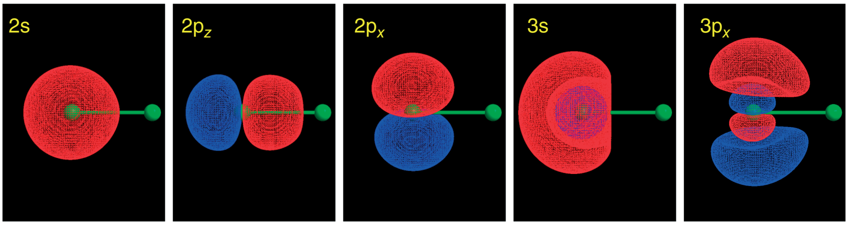

Figure 1.16 Upper panels: core and valence quasi-atomic orbitals of the FORS wave function (QUAFOs) in the N_2 molecule. Lower panels: valence quasi-atomic orbitals and two correlating quasi-atomic orbitals of a full MCSCF calculation that includes the correlating orbitals 3s, $3p_x$, $3p_y$ in the fluorine molecule (the p_y orbitals being equivalent to p_x orbitals are not shown,). For both molecules, only orbitals on one atom are shown. Note that all orbitals are *molecular* orbitals (see Section 1.3.3).

For each molecule, a panel of nine blocks of entries is displayed, each block consisting of the values for **T**, **V**, and **E**. The four corner blocks correspond to the four energies discussed in the preceding Section 1.6.1. The upper left corner corresponds to the two separated atoms. Since 2 × Energy (i) has been subtracted from all energies, this entry is always zero. The lower left corner contains the binding energy obtained using the unchanged optimal orbitals of the free atoms, i.e., it is (Energy (ii) minus 2 × Energy (i)). The upper right corner block lists the energy of the quasi-atoms in the molecule relative to the free atoms, i.e., it is 2 × (Energy (iv) minus Energy (i)). The lower right hand corner, finally, lists the actual FORS binding energy from the full MCSCF calculations, i.e., it is (Energy (iii) minus 2 × Energy (i)).

The other five blocks represent the energy *changes* between the respective adjacent blocks and their values were simply obtained by subtraction. Thus, the blocks in the *second column* show the energy differences that result from replacing the optimal free-atom orbitals by the deformed quasi-atomic orbitals of the molecule, and the blocks in the *second row of blocks* exhibit the differences between the molecular energies and the *intra-atomic* energies, i.e., the energy contributions due to the *interatomic* interactions.

Table 1.3 Energy changes from free-atom energies to molecular FORS energies, resolved in terms of intra- and interatomic contributions and in terms of free atom and deformed atomic orbitals.

Contributions to energy change		Free-atom orbitals	Orbital deformation	Quasi-atomic orbitals	Free-atom orbitals	Orbital deformation	Quasi-atomic orbitals
			H_2			B_2	
Intra-atomic contributions	T	0	397.3	397.3	0	564.6	564.6
	V	0	−355.8	−355.8	0	−507.4	−507.4
	E	0	41.5	41.5	0	57.1	57.1
Interatomic contributions	T	−167.8	−77.2	−245.0	−142.4	−325.1	−467.6
	V	58.7	−7.5	51.2	81.7	231.1	312.7
	E	−109.1	−84.7	−193.8	−60.8	−94.0	−154.8
Total binding energy	T	−167.8	320.1	152.3	−142.4	239.5	97.0
	V	58.7	−363.3	−304.6	81.7	−276.4	−194.7
	E	−109.1	−43.2	−152.3	−60.8	−36.9	−97.7
			C_2			N_2	
Intra-atomic contributions	T	0	1407.2	1407.2	0	2352	2352
	V	0	−1301.8	−1301.8	0	−2127	−2127
	E	0	105.4	105.4	0	225	225
Interatomic contributions	T	−608.0	−573.6	−1181.6	−955	−1056	−2011
	V	468.2	379.7	847.9	862	584	1446
	E	−139.8	−193.8	−333.6	−92	−472	−564
Total binding energy	T	−608.0	833.7	225.7	−955	1296	341
	V	468.2	−922.1	−453.8	862	−1543	−680
	E	−139.8	−88.4	−228.2	−92	−247	−339
			O_2			F_2	
Intra-atomic contributions	T	0	1264.9	1264.9	0	590.7	590.7
	V	0	−1119.3	−1119.3	0	−547.2	−547.2
	E	0	145.6	145.6	0	43.5	43.5
Interatomic contributions	T	−378.3	−734.8	−1113.1	−100.4	−464.1	−564.5
	V	357.2	459.3	816.4	97.2	393.3	490.5
	E	−21.2	−275.5	−296.7	−3.2	−70.8	−74.0
Total binding energy	T	−378.3	530.1	151.8	−100.4	126.7	26.3
	V	357.2	−660.0	−302.9	97.2	−153.9	−56.7
	E	−21.2	−129.9	−151.1	−3.2	−27.2	−30.4

Quadruple-zeta bases, energies in mh.

The following conclusions are manifest from these data.

1) The first column exhibits the bonding that is achieved when the free-atom orbitals are used in the molecular calculation. In all molecules, this bonding is seen to be the result of the lowering of the interatomic kinetic energy contributions that is stronger than a concomitant potential energy increase, exactly as in H_2^+ and H_2. There is no question that this binding is due to delocalization.
2) The center column in the first row of the blocks shows the *intra-atomic energy increase* when the optimal free-atom orbitals are replaced by the deformed quasi-atomic orbitals of the molecule. In all molecules, the intra-atomic *potential* energy *decreases* considerably, but the intra-atomic *kinetic* energy *increases* even more so that the total intra-atomic energy increases somewhat (as it must by the intra-atomic variation principle). These changes in the intra-atomic kinetic and potential energies show that the quasi-atomic orbital deformations are dominated by an overall contraction in all molecules, as was the case in H_2^+ and H_2.
3) The third column in the second row of the blocks shows the interatomic interactions that create the bond between the quasi-atoms calculated with the deformed quasi-atomic orbitals. These interactions are always stronger than the interactions between the undeformed atoms listed in the first column. This enhancement is indicated by blue-green highlighting of the energies in the second row of the blocks. In all molecules, as in H_2^+ and H_2, the enhancement is due to the interatomic *kinetic* contributions, which are indicated by yellow highlighting.
4) The values of the just mentioned enhancement of the interatomic interaction by quasi-atomic orbital deformation, are given in the second column of the second row of the blocks (i.e., the center block of the entire panel). It is always the result of a considerable enhancement of the interatomic *kinetic* contributions, which indicates that, the quasi-atomic orbital deformations increase the delocalization, as was discussed in detail for H_2^+ and H_2. On the other hand, the quasi-atomic orbital deformations render the interatomic *potential* contribution more antibonding in all molecules, except in H_2 where it becomes slightly less antibonding. In all systems (including H_2), the total interatomic potential energy contribution (last column, second row of the blocks) is very antibonding.
5) The lowest block in the third column shows the kinetic and potential energy decomposition of the FORS binding energy. These contributions are, respectively, positive and negative (as they must be by the virial theorem). From the data in the blocks in the first and second row of the last column, it is apparent that these signs are a consequence of the *intra-atomic orbital* contraction mentioned above, which are a side effect of the enhanced binding of the *interatomic kinetic* contributions due to orbital deformation, as has been discussed for H_2^+ and H_2.

In summary, bonding is brought about by the *kinetic energy* lowering in the *interatomic* interactions in all molecules. The kinetic energy lowering is further enhanced by a deformation of the quasi-atomic orbitals, which is an overall contraction. This enhancement prevails over the intra-atomic energy increase that is unavoidably also generated by the deformation. The intra-atomic energy increase is the result of large compensating intra-atomic kinetic and potential energy changes that cause the kinetic binding energy to be positive and the potential binding energy to be negative, but reveal no information about the origin of binding.

1.6.3
Synergism along the Dissociation Curve

The overall consistency that has been found for the essential bonding contributions at the equilibrium geometries extends to the entire dissociation curves. This similarity is exhibited in Figures 1.17–1.19 for the molecules B_2, C_2, N_2, O_2, and F_2. Each molecule is represented by one row of panels. In each row, from left to right:

- The first panel displays the kinetic, potential, and total energy curves for the *interatomic interactions obtained with the free-atom orbitals* (corresponding to item 1) in the preceding Section 1.6.2).
- The second panel displays the curves for the *interatomic interactions obtained with the deformed quasi-atomic orbitals of the molecules, that is, the QUAFOs* (corresponding to item 3) in the preceding Section 1.6.2).
- The third panel displays the curves for the *intra-atomic* energy changes caused by the deformations that change the free-atom orbitals into the QUAFOs (corresponding to item 2) in the preceding Section 1.6.2).
- The fourth panel shows the binding curves obtained by optimizing the QUAFOs at each internuclear distance (corresponding to item 5) in the preceding Section 1.6.2). The values of this FORS binding energy curve, as well as its kinetic and potential components in the fourth panel, are the sums of the corresponding values in the second and third panels.

Between the equilibrium distance, which is indicated by a gray vertical line, and infinite separation, the curves of all molecules exhibit the same overall pattern, namely:

Binding is provided by the *interatomic* interactions (first and second panel), specifically by the *kinetic* interatomic energy lowering, due to delocalization, prevailing over an interatomic potential energy increase, presumably due to charge accumulation in the bond and sharing coulombic effects. The interatomic interactions for the deformed quasi-atomic orbitals (second panel) are qualitatively similar to those for the undeformed free-atom orbitals (first panel). But the deformations enhance these contributions.

The *intra-atomic* contribution is the result of a large increase in the kinetic component prevailing slightly over a large decrease in the potential component,

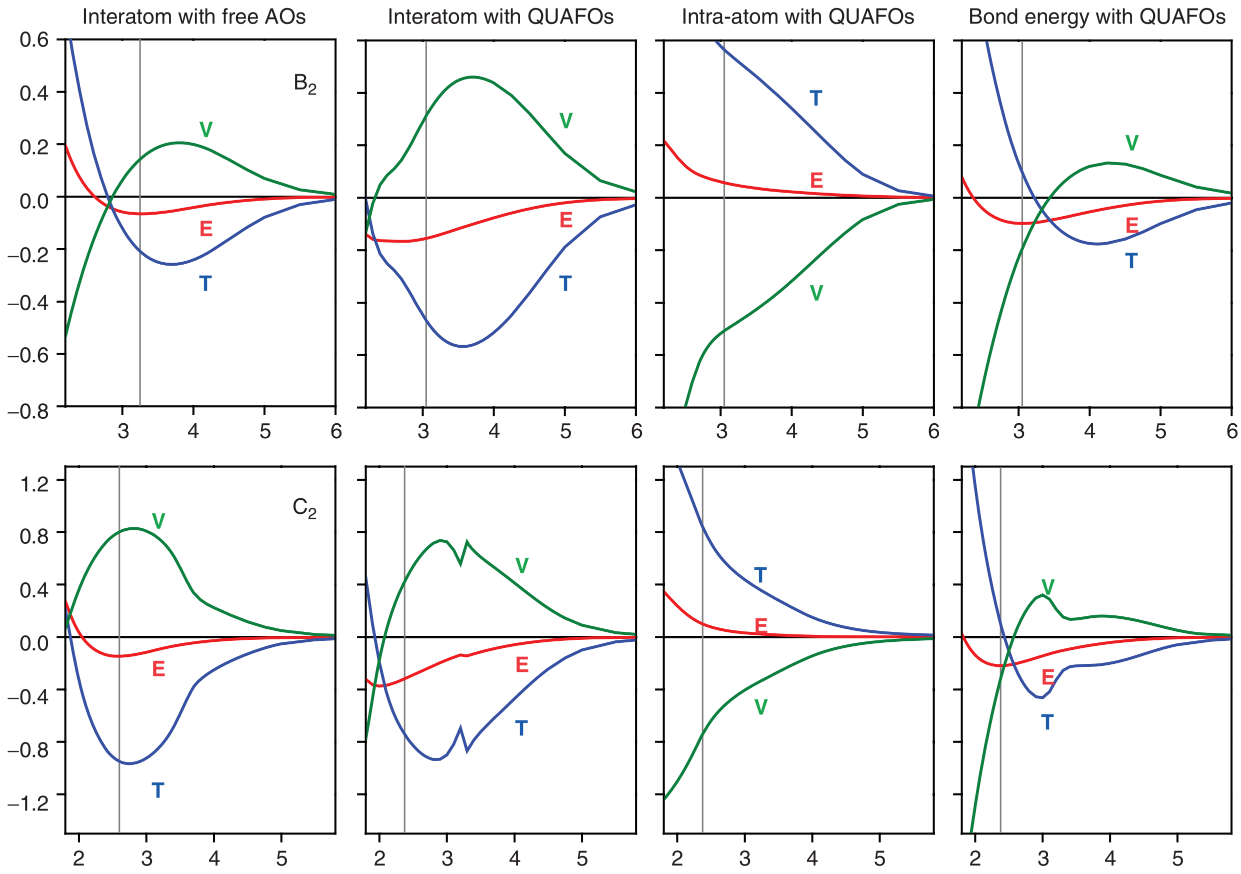

Figure 1.17 Contributions to kinetic, potential, and total binding energy curves of B_2 (first row of panels) and C_2 (second row of panels) for full valence space wave functions. First column of panels: *interatomic* contributions when the quasi-atomic orbitals are the optimized orbitals of the free atoms. Second column of panels: *interatomic* contributions when the quasi-atomic orbitals are the QUAFOs of the FORS wave function. Third column of panels: *intra-atomic* contributions due to deformation of the free-atom orbitals into QUAFOs. Fourth column of panels: FORS binding energy curves. Internuclear distance in Bohr. Energies in hartree.

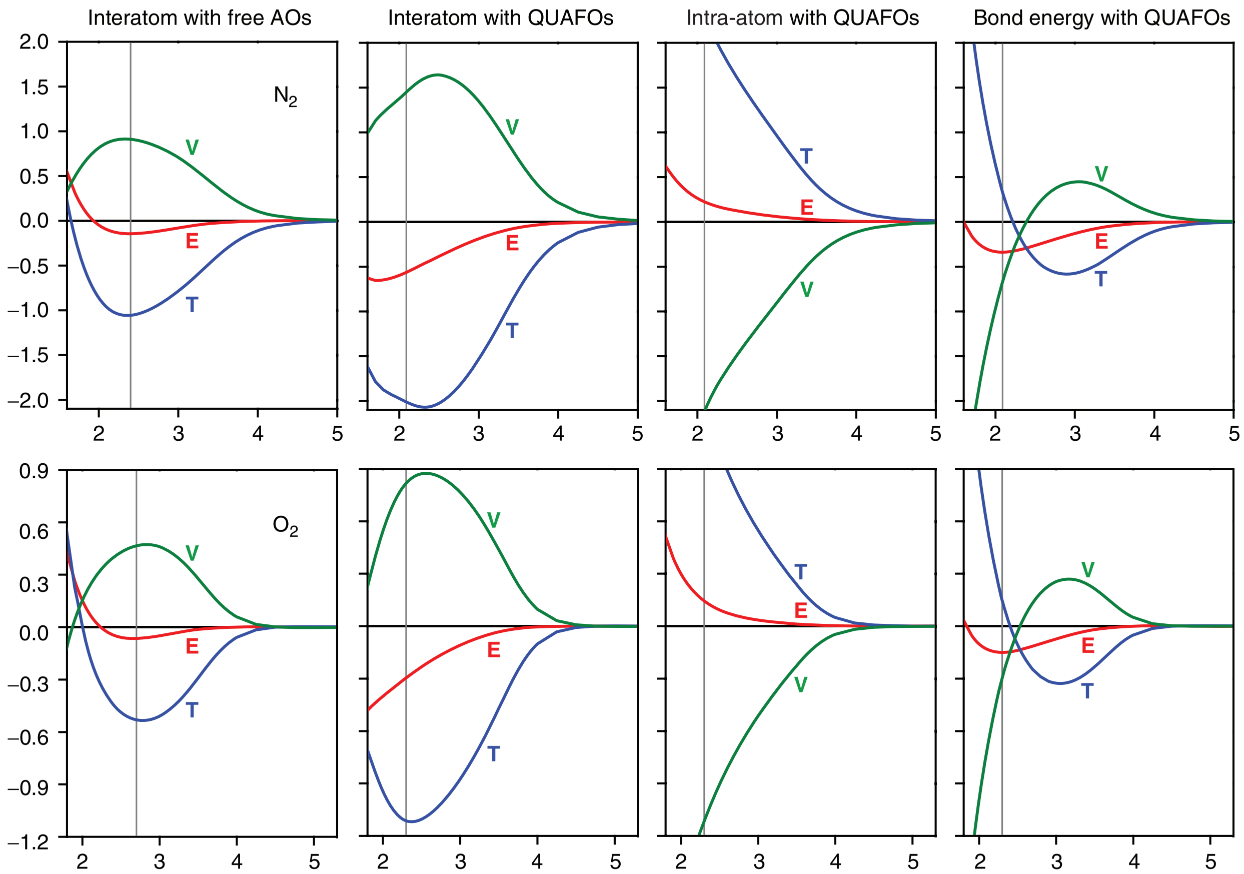

Figure 1.18 Contributions to kinetic, potential and total binding energy curves of N_2 (first row of panels) and O_2 (second row of panels) for full valence space wave functions. See caption of Figure 1.17 for a description of the column of panels.

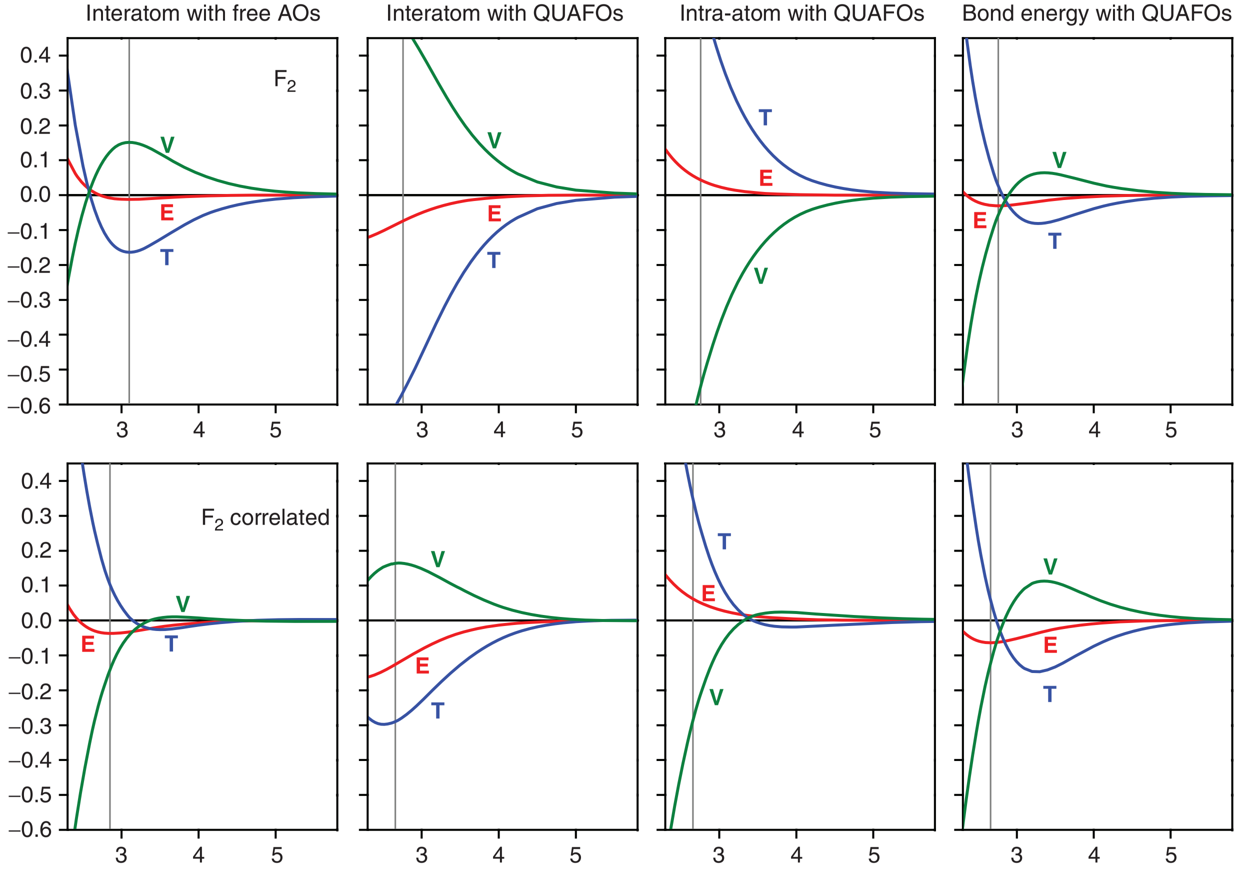

Figure 1.19 Contributions to kinetic, potential, and total binding energy curves of F_2. The first row of panels contains the data of the FORS calculations. The second row of panels contains the results of a full MCSCF calculation including, in addition, the correlating orbitals 3s, $3p_x$, $3p_y$ on both atoms (see Figure 1.16). See caption of Figure 1.17 for the description of the column of panels.

changes that imply intra-atomic contraction. Although the intra-atomic changes determine the signs of the kinetic and components of the binding energy, they yield an overall antibonding contribution to this energy.

It is evident that, in all of these molecules, the basic synergism that leads to covalent binding is entirely analogous to the one that was found for H_2^+ and H_2 and exhibited in Figures 1.9 and 1.13.

Parenthetically, it is noted that the kinks in the curves for C_2 are due to the avoided curve crossing that exists in this system. The curve shown is the lowest ${}^1\Sigma_g{}^+$ state obtained from a state-average MCSCF calculation over the three lowest states $X^1\Sigma_g{}^+$, $B'^1\Sigma_g{}^+$, $B^1\Delta_g$ (even though the Δ-state is lower at large distances). Appropriately corresponding state averaged calculations were performed for the carbon atom to obtain the dissociation limit of the lowest ${}^1\Sigma_g{}^+$ state.

1.6.4
Effect of Dynamic Correlation on Covalent Binding

The effect of dynamic electron correlation on the bond in the H_2 molecule was discussed in Section 1.5.6. In that case, it accounted for about 13% of the binding energy and it did not change the conclusions regarding the origin of covalent binding. It was also noticed that the energy lowering achieved by the correlating adjustments in the wave function are not able to compensate entirely for the adverse effect that electron repulsion has on bond formation at the FORS level through the sharing coulombic interaction.

The molecules treated in the present section differ from H_2 in that dynamic electron correlation already exists in the separate atoms. It is generally found that dynamic correlation in a molecule is larger than the sum of the dynamic correlations in the separate atoms, presumably because there is more space available for the electrons to avoid each other in the molecule than in the separate atoms. The data in the first three rows in Table 1.4 confirm this general trend for the molecules treated in the present section by furnishing a comparison of the FORS binding energies with the experimental binding energies (The experimental energy for B_2 is from Bytautas *et al.* [30] the others are from Feller and Sordo [31]). It can

Table 1.4 Dynamic correlation contributions to bond energies (mh).

	H_2	B_2	C_2	N_2	O_2	F_2
D_e FORS	−152.3	−97.7	−228.2	−339	−151.1	−30.4
D_e Experiment	−174.5	−107.9[a]	−230.1[b]	−364.1[b]	−191.6[b]	−60.9[b]
% Dynamic correlation	13	9.5	0.8	7	21	50
D_e FORS+[c]			−228.2	−360.5	−192.5	−63.9

[a] From Bytautas *et al.*, Ref. [30]

[b] From Feller and Sordo, Ref. [31]

[c] See second and third but last paragraphs of Section 1.6.4.

be inferred that the bonds in B_2, C_2, N_2, O_2 are dominated by covalent bonding of the FORS wave functions, that is, by the interactions in the orbital space of the (optimized) minimal basis sets, which are the ones that were analyzed in the preceding sections.

In F_2, on the other hand, about half of the binding energy is due to a lowering of the dynamic correlation energy upon molecule formation. This does not invalidate the analysis of the FORS wave function in the preceding sections, which elucidates that part of the binding that is the result of the interactions within the orbital space of the minimal basis sets.

Remarkably, the binding energy is recovered within 3 mh when the dynamic correlation is simply accounted for by an extended MCSCF calculation that provides one correlating orbital for each of the six valence orbitals containing lone pairs. These correlating orbitals were shown in the lower panel set in Figure 1.16. The second row of Figure 1.19 exhibits the resolution of the dissociation curve obtained with this wave function in terms of contributions that are analogous to those formulated in Sections 1.6.3 and 1.6.4. It is apparent that even in this case, the basic pattern of the interatomic and intra-atomic contributions is the same as that obtained for the FORS wave function, which is shown in the first row of that figure.

In fact, analogous MCSCF calculations, based on wave functions with N valence electrons in N valence orbitals, yield good binding energies for N_2 and O_2 as well, as shown in the last row of Table 1.4, where they are denoted as FORS+ calculations.[2] For the C_2 molecule, the minimal basis set FORS wave function provides already one orbital for each electron and this is presumably the reason why, here, the FORS calculation recovers the binding energy within 3.5 mh. All of these energies were calculated at the optimized equilibrium geometries.

A more extreme case is presented by the molecule Be_2, which would not exist without the help of the dynamic correlation interactions. However, as the detailed analysis of this bond by the present authors [32] showed, even in this case the contributions of the minimal basis set interference interactions are in fact essential for the existence of the bond.

1.7
Conclusions

As Robert Mulliken noted in the remark quoted at the beginning of this chapter, chemical bonding is more complicated than one would like it to be – a not uncommon experience in the sciences. The following précis summarizes the essential conclusions regarding covalent binding that emerge from the detailed analyses of the seven molecules examined in the preceding sections.

---

[2] For the O_2 molecule, 14 orbitals are used, that is, the additional 3s, $3p_x$, $3p_y$ (but not $3p_z$) orbitals are added. This is because the separated atom calculation must be performed in cylindrical symmetry, which is done by a state-averaged MCSCF calculation involving the p_x as well as the p_y orbital.

1) Electronic ground states in atoms and molecules are determined by the optimal compromise in the variational competition between the electrostatic potential pulling the electrons toward the nuclei and the intrinsic kinetic delocalization drive of electron waves, which resists localization toward nuclei. Bonding occurs when the molecule offers a variational compromise with an energy lower than that available in the separated atoms.
2) The formation of a covalent bond is a consequence of the *kinetic energy lowering* that results from valence electrons *delocalizing* over several atoms. Such delocalization occurs between open-shell atoms, that is, atoms in which the number of valence electrons is less than twice the number of valence-shell *minimal basis set* orbitals, because some valence electrons can then exploit valence orbitals on *several* atoms by partial occupation.

   The delocalization is manifest when electronic wave functions are expressed in terms of delocalized bonding orbitals. When the wave functions are equivalently expressed in terms of quasi-atomic orbitals, then the kinetic energy lowering through delocalization is quantified by the negative *interference energy* between the quasi-atomic orbitals involved in the delocalization.3)
3) The *kinetic* energy lowering through delocalization prevails over a lesser *potential energy increase* that is caused by the accumulation of charge in the bond region, which is associated with delocalization.4)
4) At and near the equilibrium distance, delocalization has the special feature that it is *enhanced by shrinkage of the quasi-atomic wave function components* toward their respective nuclei.5) This additional interatomic delocalization is therefore coupled with *contractions of the quasi-atomic orbitals*, whereby electronic charge is moved *from the outer regions* into the *interatomic* region as well as into the *intra-atomic* regions. The resulting energy lowering involves the following subtle interplay between *interatomic* and *intra-atomic* energy changes.

   The charge shift into the bond region enhances the *interatomic* delocalization and thereby lowers the kinetic energy further. Moreover, this *interatomic* kinetic energy lowering weakens the *overall* kinetic resistance against localization and thereby allows the nuclear attractions to pull more electronic charge toward the nuclei. As a result, the *intra-atomic potential* energy strongly decreases and the *intra-atomic kinetic* energy strongly increases until the virial ratio $2\mathbf{T} = |\mathbf{V}|$ is reached, which characterizes the optimal compromise in the variational competition between kinetic and potential energy at the equilibrium distance.6)

   Even though the shift of charge into the *intra-atomic* region is thus instrumental in bringing about the compliance with the *overall* virial constraint, the *total intra-atomic energy nonetheless increases* in accordance with the *intra-atomic*

---

3) Interference energies are conceptually related to the resonance energies of molecular orbital and valence bond theories. However, the resolution of resonance energies into kinetic and potential components was never examined.

4) Charge accumulation in the bond *does not lower* the potential energy! See Section 1.4.5.3.

5) Even though the atomic contractions decrease the overlap integral! See Sections 1.4.3 and 1.4.5.5.

6) In accordance with the fundamental analysis in Section 1.2.3.

variation principle (the intra-atomic kinetic energy increase being stronger than the intra-atomic potential energy decrease). This *intra-atomic* energy increase is however less than the *interatomic* kinetic energy decrease through the increased delocalization that drives the contractions.

5) At larger internuclear distances the contraction discussed under item 4) does not occur and the delocalization discussed under items 2) and 3) is the only contributor to covalent bonding.[7)]

6) The detailed changes in the *potential* interactions that occur when bonds form are involved and complicated to sort out. It is found, however, that the *total contribution of all interatomic potential interactions* is positive, that is, antibonding in all molecules at all internuclear distances.

   The negative sign of the potential contribution to the total binding energy at the equilibrium geometry is the result of the intra-atomic adjustments discussed in the second paragraph of item 4) above. Since these *intra-atomic* adjustments are consequences of the *interatomic* kinetic energy attenuation, the sign of this potential contribution does not indicate what drives bond formation.[8)]

7) In as much as delocalization and kinetic energy changes are *one-electron* attributes, covalent bonding is the cumulative result of the bonding effects of the individual bonding electrons. The *interelectronic interactions* have an adverse effect on covalent bonding for the following reason.

   The delocalization of several electrons over several atoms increases the interpenetration of the respective electron clouds and, hence, strengthens the electrostatic repulsions between them, which diminishes the bond energy compared to what it would be without electron–electron interaction. This detrimental effect is mitigated, in so far as possible, by the inclusion of dynamic correlation terms in the wave function. In some molecules, dynamic correlation contributes a considerable part of the bonding energy. Nonetheless, the kinetic effects of delocalization are always essential for covalent bonding.

8) Finally, it should be noted that covalent bonding is not the only kind of chemical bonding. As Schwarz and coworkers have pointed out [12w, 33], changes in each of the terms in the electronic energy expression, viz in the kinetic terms, in the nuclear–electronic interactions, and in the electron–electron interactions can result in bonding. While covalent bonding is driven by changes in the kinetic terms, ionic bonding and long-range multipole interactions are driven by changes in the electron–nuclear interactions. Long-range dispersion forces, on the other hand, are driven by changes in the electron–electron interactions [34].

[7)] This is related to the less stringent form of the virial theorem in this region. See Section 1.2.3.

[8)] That the actual values of the kinetic and potential energies *at the variational minimum* generally do not provide sufficient information to deduce the physical origin of energy differences between systems was discussed in detail in the last paragraph of Section 1.2.2.

Acknowledgments

This work was supported in part by the US Department of Energy, Office of Basic Energy Sciences, Division of Chemical Sciences, Geosciences and Biosciences at the Ames Laboratory (for K.R.). The Ames Laboratory is operated for the US Department of Energy by Iowa State University under Contract DE-AC02-07CH11358. The work was supported in part by the National Science Foundation under Grant CHE-1147446 to Iowa State University (for M.W.S.). The work was supported in part with federal funds from the National Cancer Institute, National Institutes of Health, under Contract No. HHSN 261200800001E (for J.I.). The content of this publication does not necessarily reflect the views or policies of the Department of Health and Human Services, nor does mention of trade names, commercial products, or organizations imply endorsement by the US Government.

References

1. References to literature on the early history can be found in the article Ruedenberg, K. and Schwarz, W.H.E. (2013) Three millennia of atoms and molecules, in *Proceedings of the Symposium Pioneers in Quantum Chemistry* (eds T. Strom and A. Wilson), American Chemical Society, Washington, DC.
2. See, e.g., Helmholtz' Faraday address of 1881 at the Royal Institution in London, as reported on pp.278 to 284 in Volume II of Koenigsberger, L. (1902) *Hermann von Helmholtz*, Vieweg, Braunschweig.
3. Abegg, R. (1904) *Z. Anorg. Chem.*, **39**, 30.
4. Kossel, W. (1916) *Ann. Phys.*, **49**, 229.
5. Lewis, G.N. (1916) *J. Am. Chem. Soc.*, **38**, 762; and in the book *Valence and the Structure of Atoms and Molecules*, ACS Sponsored Monograph by the Chemical Catalog Company, 1923; republished by Dover, New York, 1966.
6. Heitler, W. and London, F. (1927) *Z. Phys.*, **44**, 455.
7. Burreau, Ø. (1927) *Det. Kgl. Danske Vid. Selskab.*, **7**, 1.
8. James, H.M. and Coolidge, A.S. (1933) *J. Chem. Phys.*, **1**, 825.
9. Slater, J.C. (1933) *J. Chem. Phys.*, **1**, 687.
10. Hellmann, H. (1933) *Z. Phys.*, **35**, 180, In his book *Quantenchemie*, Deuticke, Vienna, 1937, Hellmann seems to be more troubled about the apparent contradiction to the virial theorem.
11. (a) Ruedenberg, K. (1962) *Revs. Mod. Phys.*, **34**, 326. (b) Edmiston, C. and Ruedenberg, K. (1964) *J. Phys. Chem.*, **68**, 1628. (c) Feinberg, M.J., Ruedenberg, K., and Mehler, E. (1970) in *Advances in Quantum Chemistry*, vol. 5 (ed. P.O. Löwdin), Academic Press, p. 27. (d) Feinberg, M.J. and Ruedenberg, K. (1971) *J. Chem. Phys.*, **54**, 1495. (e) Feinberg, M.J. and Ruedenberg, K. (1971) *J. Chem. Phys.*, **55**, 5804. (f) Ruedenberg, K. (1975) in *Localization and Delocalization in Quantum Chemistry*, vol. 1 (ed. R. Daudel), Reidel Publishing Company, Dordrecht, p. 222.
12. (a) Goddard, W.A. and Wilson, C.W. (1972) *Theor. Chim. Acta*, **26**, 195 and 211. (b) Kutzelnigg, W. (1973) *Angew. Chem.*, **85**, 551 and *Angew. Chem. Int. Ed.*, **12**, 46. (c) Steiner, E. (1975) *The Determination and Interpretation of Molecular Wave Functions*, Cambridge University Press. (d) Fukui, K. (1976) *Chemical Reactions and Electronic Orbitals*, Maruzen Co, Tokyo, in Japanese only (*Kagaku Hannoh to Denshi no Kidoh*). (e) Mulliken, R.S. and Ermler, W.C. (1977) *Diatomic Molecules*, Section II.F, Academic Press, New York. (f) Harcourt, R.D., Solomon, H., Beckworth, J., and Chislett, L. (1982) *Am. J. Phys.*, **50**, 557. (g) Rozendahl, A. and Baerends, E.J. (1985) *Chem.*

Phys, **95**, 57. (h) Baird, N.C. (1986) *J. Chem. Educ.*, **63**, 660. (i) Harcourt, R.D. (1988) *Am. J. Phys.*, **56**, 660. (j) Nordholm, S. (1988) *J. Chem. Educ.*, **65**, 581. (k) Kutzelnigg, W. (1990) in *The Concept of the Chemical Bond*, vol. 2 (ed. Z.B. Maksic), Springer, Berlin, p. 1. (l) Harris, F.E. (1991) in *Encyclopedia of Physics*, 2nd edn (eds R.G. Lerner and G.L. Trig), John Wiley & Sons, Inc., New York, p. 762. (m) Melrose, M.P., Chauhan, M., and Kahn, F. (1994) *Theor. Chim. Acta*, **88**, 311. (n) Rioux, F. (1997) *Chem. Educ.*, **2** (6), 1. (o) Bacskay, G.B., Reimers, J.R., and Nordholm, S. (1997) *J. Chem. Ed.*, **74**, 1494. (p) Gordon, M.S. and Jensen, J.H. (1998) in *Encyclopedia of Computational Chemistry* (ed. P.v.R. Schleyer), John Wiley & Sons, Inc., New York, pp. 3198–3214. (q) Gordon, M.S. and Jensen, J.H. (2000) *Theor. Chem. Acc.*, **103**, 248. (r) Bickelhaupt, F.M. and Baerends, E.J. (2000) *Rev. Comput. Chem.*, **15**, 1. (s) Rioux, F. (2001) *Chem. Educ.*, **6** (5), 288. (t) Cardozo, T.M. and Nascimento, M.A.C. (2009) *J. Chem. Phys.*, **130**, 104102. (u) Cardozo, T.M. and Nascimento, M.A.C. (2009) *J. Phys. Chem. A*, **113**, 12541. (v) Cardozo, T.M., Nascimento Freitas, G., and Nascimento, M.A.C. (2010) *J. Phys. Chem. A*, **114**, 8798. (w) Bitter, T., Wang, S.G., Ruedenberg, K., and Schwarz, W.H.E. (2010) *Theor. Chem. Acc.*, **127**, 237. (x) Fantuzzi, F., Cardozo, T.M., and Nascimento, M.A.C. (2012) *Phys. Chem. Chem. Phys.*, **14**, 5479.

13. (a) Ruedenberg, K. and Schmidt, M.W. (2007) *J. Comput. Chem.*, **28**, 391. (b) Ruedenberg, K. and Schmidt, M.W. (2009) *J. Phys. Chem. A*, **113**, 1954.

14. Bacskay, G.B. and Nordholm, S. (2013) *J. Phys. Chem. A*, **117**, 7946–7958.

15. (a) Coulson, C.A. and Bell, R.P. (1945) *Trans. Faraday Soc.*, **41**, 141. (b) Löwdin, P.O. (1959) *J. Mol. Spectrosc.*, **3**, 46.

16. The word "stock" is being used with the meaning it has in horticulture, notably in arboriculture and viticulture. See, e.g., Mudge, K., Janick, J., Scofield, S., and Goldschmidt, E.E. (2009) A history of grafting. *Horticultural Rev.*, **35**, 9, *http://www.hort.purdue.edu/newcrop/janick-papers/c09.pdf* (accessed on 22 November 2013).

17. (a) Ruedenberg, K., Schmidt, M.W., Gilbert, M., and Elbert, S.T. (1982) *Chem. Phys.*, **71**, 41. (b) Ruedenberg, K., Schmidt, M.W., and Gilbert, M. (1982) *Chem. Phys.*, **71**, 51. (c) Ruedenberg, K., Schmidt, M.W., Gilbert, M., and Elbert, S.T. (1982) *Chem. Phys.*, **71**, 65.

18. West, A., Schmidt, M.W., Gordon, M.S., and Ruedenberg K. (2013) *J. Chem. Phys.*, **139**, 234107.

19. (a) Lu, W.C., Wang, C.Z., Schmidt, M.W., Bytautas, L., Ho, K.M., and Ruedenberg, K. (2004) *J. Chem. Phys.*, **120**, 2629. (b) Lu, W.C., Wang, C.Z., Schmidt, M.W., Bytautas, L., Ho, K.M., and Ruedenberg, K. (2004) *J. Chem. Phys.*, **120**, 2638. (c) Lu, W.C., Wang, C.Z., Chan, T.L., Ruedenberg, K., and Ho, K.M. (2004) *Phys. Rev. B*, **70**, 04110(R).

20. (a) Ivanic, J., Atchity, G.J., and Ruedenberg, K. (2008) *Theor. Chem. Acc.*, **120**, 281. (b) Ivanic, J. and Ruedenberg, K. (2008) *Theor. Chem. Acc.*, **120**, 295.

21. The most accurate value reported for the equilibrium distance so far is 1.9971933199699992 bohr with an energy of −0.6026346191065398 hartree by Scott, T.C., Aubert-Frecon, M., and Grotendorst, J. (2006) *Chem. Phys.*, **324**, 323.

22. Newton, I. *Philosophiae Naturalis Principia Mathematica*, London, 1687; Book I, Section XII.

23. Finkelstein, B.N. and Horowitz, G.E. (1928) *Z. Phys.*, **48**, 118.

24. Kolos, W. (1994) *J. Chem. Phys.*, **101**, 1330.

25. Nakatsuji, H. (2004) *Phys. Rev. Lett.*, **93**, 030403.

26. This is the theoretical value of Cencek, W. and Szalewicz, K. (2008) *Int. J. Quantum Chem.*, **108**, 2191. The corresponding energy is −1.174475714 hartree.

27. Schmidt, M.W., Ivanic, J., and Ruedenberg K. in preparation.

28. Dunning, T.H. (1989) *J. Chem. Phys.*, **90**, 1007. A survey of cc-type basis sets is given at the website *http://tyr0.chem.wsu.edu/~kipeters/Pages/*

cc˙append.html (accessed 22 September 2013).

29. (a) Schmidt, M.W., Baldridge, K.K., Boatz, J.A., Elbert, S.T., Gordon, M.S., Jensen, J.H., Koseki, S., Matsunaga, N., Nguyen, K.A., Su, S., Windus, T.L., Dupuis, M., and Montgomery, J.A. (1993) *J. Comput. Chem.*, **14**, 1347. (b) Gordon, M.S. and Schmidt, M.W. (2005) in *Theory and Applications of Computational Chemistry, the First Forty Years* (eds C.E. Dykstra, G. Frenking, K.S. Kim, and G.E. Scuseria), Elsevier, Amsterdam, pp. 1167–1189.
30. Bytautas, L., Matsunaga, N., Scuseria, G.E., and Ruedenberg, K. (2012) *J. Phys. Chem. A*, **116**, 1717.
31. Feller, D. and Sordo, J.A. (2000) *J. Chem. Phys.*, **113**, 485.
32. Schmidt, M.W., Ivanic, J., and Ruedenberg, K. (2010) *J. Phys. Chem. A*, **114**, 8687.
33. Bitter, T., Ruedenberg, K., and Schwarz, W.H.E. (2007) *J. Comput. Chem.*, **28**, 411.
34. See e.g., (a) Buckingham, A.D., Fowler, P.W., and Hudson, J.M. (1988) *Chem. Rev.*, **88**, 963. (b) Chałasiński, G. and SzczJśniak, M.M. (2000) *Chem. Rev.*, **100**, 4227. (c) Stone, A.J. (1996) *The Theory of Intermolecular Forces*, Clarendon, Oxford.